
# DETONATION PROPAGATION THROUGH DUCTS IN A PULSED DETONATION ENGINE

THESIS

Jeffrey M. Nielsen, Capt, USAF

AFIT/GAE/ENY/11-M21

**DEPARTMENT OF THE AIR FORCE**
**AIR UNIVERSITY**

**AIR FORCE INSTITUTE OF TECHNOLOGY**

**Wright-Patterson Air Force Base, Ohio**

AFIT/GAE/ENY/11-M21

# DETONATION PROPAGATION THROUGH DUCTS IN A PULSED DETONATION ENGINE

THESIS

Presented to the Faculty

Department of Aeronautics and Astronautics

Graduate School of Engineering and Management

Air Force Institute of Technology

Air University

Air Education and Training Command

In Partial Fulfillment of the Requirements for the

Degree of Master of Science in Aeronautical Engineering

Jeffrey M. Nielsen

Capt, USAF

March 2011

AFIT/GAE/ENY/11-M21

# DETONATION PROPAGATION THROUGH DUCTS IN A PULSED DETONATION ENGINE

Jeffrey M. Nielsen

Capt, USAF

Approved:

| | |
|---|---|
| _____ | _____ |
| Paul I. King (Chairman) | Date |
| _____ | _____ |
| Frederick R. Schauer (Member) | Date |
| _____ | _____ |
| Mark F. Reeder (Member) | Date |

## Abstract

A study of configurations to allow a consistent and predictable transition of a detonation from one detonation tube to another is presented for the development of a continuously operating pulsed detonation engine (PDE). A PDE without a high energy ignition system or a deflagration-to-detonation transition (DDT) device will have increased efficiency, reduced cost, improved performance, and reduced overall vehicle weight. The intent of this study was to visualize detonation propagation through a cross-over tube; to minimize energy losses of a detonation wave through a cross-over tube; and to determine the mechanisms that relate to directly initiating a detonation via tube-to-tube initiation. Detonation tube cross-over width, cross-over geometry and fuel were varied to determine their effect on initiation via a cross-over tube. Velocities within 15% of the upper Chapman-Jouguet (CJ) point are desired and indicate successful detonations. The studied detonations decoupled entering and exiting the cross-over tube due to diffraction at the boundaries of the cross-over tube. High-speed schlieren imaging showed that the mechanism of shock reflection could be used to transition the combustion back to a detonation within two detonation tube diameters of the cross-over tube exit.

**Acknowledgements**

I would first like to thank Dr. Schauer and AFRL/RZTC for providing the funding and motivation for this research. I can honestly say that I had a lot of fun with this project and that is in large part due to the atmosphere Dr. Schauer has built in his lab. I am grateful for the opportunity I had to work in the machine shop, designing, building and fabricating, as well as in the control room taking data.

This research and the results presented in this document would be only wishful thinking if it were not for Chris Stevens. Chris unselfishly gave of his time and knowledge to answer every question I had, help with any setup I needed and look for any information I had forgotten. His patience with the schlieren optics is the reason our images turned out as good as they did.

Curt Rice was the PDE operator for nearly every run documented here and was always willing to help in any way he could. He helped setup, tear down, trouble-shoot, re-configure and anything else that needed to be done to get the results we needed. I am truly thankful for his assistance and willingness to help.

The man responsible for putting the test section together along with the geometries was Justin Goffena. Justin was able to weld all of the small pieces together and still get a bolt to fit through each of the 64 holes. He was always willing to help which was greatly appreciated.

I must also thank my advisor, Dr. King, who has made me a better engineer over the past 18 months. Whether it was in the class room or thesis work, Dr. King always held me, along with his other students, to the highest standard. He always kept those standards and pushed me to meet them every time, for that I am thankful and appreciative.

Finally, to the crew that has kept me laughing and gotten me through the homework, long days and everything else here at AFIT, I thank you and am lucky to call you all friends. Doug, Isseyas, Collin, Adam, Mike, Bob, Jared, Josh, you guys are awesome!

Jeff Nielsen

## Table of Contents

## Table of Contents (continued)

## List of Figures

Page

Page

## List of Tables

## Nomenclature

| | |
|---|---|
| b | Bias error |
| $c_p$ | Specific heat for constant pressure [J/kg-K] |
| CJ | Chapman-Jouguet |
| DDT | Deflagration to detonation Transition |
| $E_{DID}$ | Critical initiation energy [J] |
| $\dot{m}$ | Mass flow rate [kg/s] |
| p | Precision error |
| P | Pressure [Pa] |
| PDE | Pulsed Detonation Engine |
| q | Heat addition [J/kg] |
| R | Specific gas constant [J/kg-K] |
| T | Temperature [K] |
| u | Velocity [m/s] |
| U | Total measurement uncertainty |
| ws | Wave speed |
| x | Direction of travel |
| $\gamma$ | Ratio of constant specific heats |
| $\lambda$ | Cell size [cm] |
| $\nu$ | Specific volume [$m^3$/kg] |
| $\rho$ | Density [kg/$m^3$] |
| $\sigma$ | Standard deviation |
| $\varphi$ | Equivalence Ratio |

# DETONATION PROPAGATION THROUGH DUCTS IN A PULSED DETONATION ENGINE

## I. Introduction

A Pulsed Detonation Engine (PDE) is a tube, or set of tubes, coupled with a valving system at one end and open at the other end. The tubes are filled with a combustible mixture and ignited to create a detonation. The high pressure behind the detonation wave and the rapid expulsion of products out the open end produce thrust[1], Eq. (1). The fundamental difference between a PDE and a conventional engine such as an automotive or jet engine is the nature of the combustion. A detonation travels in the low hypersonic region (Mach number = 5) at 13-50 times the atmospheric pressure. In contrast, a conventional engine utilizes deflagration, which travels at low subsonic speeds (Mach number = .03) and nearly constant pressure.[2] Because of the high exhaust velocities of a PDE and the ability to size the detonation tubes for the desired thrust, pulsed detonation engines provide the potential for a low cost and comparatively simple solution for vehicles operating from static to hypersonic speeds while maintaining efficiencies better than conventional jet engines.

$$T = u_e \dot{m} + (P_e - P_a) A_e \tag{1}$$

A PDE operating cycle has three phases: fill, fire, and purge (Fig.1). In the fill phase, a fuel and air mixture enters the detonation tube. During the fire phase ignition and detonation occur and thrust is produced. Purge, the final phase, rids the detonation tube of combustion products and cools the detonation tube with pure air. Based on the PDE cycle, specific nomenclature is introduced and defined as Eqs. 2–5.

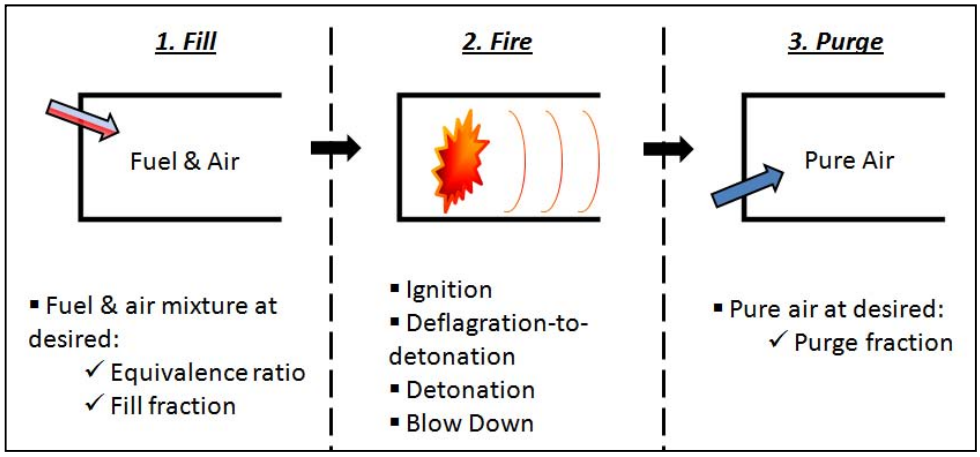


Figure 1. Three phases of the PDE cycle

$$Purge\ fraction = \frac{Volume\ of\ purge\ air\ charge}{Volume\ of\ detonation\ tube} \tag{2}$$

$$Fill\ fraction = \frac{Volume\ of\ fuel/air\ mixture\ charge}{Volume\ of\ detonation\ tube} \tag{3}$$

$$Equivalence\ ratio\ =\ \varphi = \frac{fuel\ to\ oxidizer\ ratio}{fuel\ to\ oxidizer\ ratio\ (stoichiometric)} \tag{4}$$

$$Spark\ Delay = Time\ from\ close\ of\ fill\ valves\ to\ spark\ discharge \tag{5}$$

The creation of a detonation is not a trivial task. Currently there are three common methods used to create a detonation wave. The three methods are: spark (or other energy source) inducing natural deflagration to detonation transition (DDT), use of a pre-detonator, and direct initiation. DDT begins with a deflagration, a subsonic flame, which is made turbulent by well-placed obstacles and accelerates until it becomes a detonation traveling at the local speed of sound; a pre-detonator creates a detonation in a small tube, which then transitions into a larger detonation tube; and direct initiation introduces an amount of energy larger than the

critical initiation energy of the combustible mixture, creating a detonation.

Operationally each method is not equal. The advantages and disadvantages are compared in Table 1. DDT devices suffer drag losses[3], require longer tube lengths and have less efficient combustion prior to transition to a detonation. The pre-detonator requires high chamber pressures and storage of its oxidizers (i.e. $O_2$, $NO_2$, etc.). Direct initiation requires large amounts of energy that must be released quickly. Some type of high energy system will be required to store or generate this energy charge. All three suffer increased vehicle weight during operation due to additional tube length or systems needed for DDT, pressurization, fuel storage, energy storage or energy generation.

Table 1. Tradeoffs of detonation initiation methods

| **Method** | | **Advantages** | **Disadvantages** |
|---|---|---|---|
| 1. | Deflagration-to-Detonation transition (DDT) | Relatively simple, well studied | Drag losses, less efficient combustion, weight |
| 2. | Pre-detonator | No drag losses, detonation created | Transition to detonation tube, oxidizer storage, pressurization, weight |
| 3. | Direct initiation | Detonation created, more efficient than DDT | High energy device required, weight |
| 4. | Tube-to-tube initiation | No additional systems, More efficient than DDT | Sustaining detonation through cross-over tube |

The disadvantages just described have led to the creation of a fourth method of initiation called tube-to-tube initiation. Tube-to-tube initiation combines the advantages of the above methods without the disadvantages of the above methods (Table 1). With tube-to-

tube initiation a detonation is created by one of the first three methods listed in Table 1. The detonation then travels through a cross-over tube that connects the initial detonation tube to an adjacent tube in the firing sequence. In this manner each successive tube is initiated by the previous tube and a detonation is created only once for the duration of PDE operation. Initiation of the first tube in the sequence is maintained by a cross-over tube from the last tube to fire.

Efficiency of tube-to-tube initiation is greater than other methods as the energy needed for detonation initiation is only expended once and vehicle weight is reduced as no extra systems are needed. Furthermore, the entire detonation tube can now be used to produce thrust, with none of the tube volume and fuel wasted on detonation initiation. Tube-to-tube initiation has been successfully demonstrated experimentally with two, three and four tube set-ups.[4,5] The one disadvantage of tube-to-tube initiation is the difficulty of sustaining a detonation through the cross-over tube.

The goal of this research is to investigate the mechanisms responsible for tube-to-tube initiation, with an emphasis on reducing losses in the cross-over tube. The propagation of a detonation from one tube to another via a cross-over tube will be visualized using schlieren photography. The cross-over tube width will be varied along with the shape of the cross-over tube to determine if different geometries help promote detonation propagation and if smaller cross-over tubes, requiring less fuel, can be developed.

## II. Background and Theory

### 1. Previous Research

The simplicity and added efficiency of tube-to-tube initiation are clearly attractive to the development of an operational PDE. Tube-to-tube initiation requires that a detonation be split and redirected from the initial propagation direction. To that end, the following work has been done to determine if redirecting and splitting a detonation into multiple detonation fronts is possible.

Studies show that detonations can propagate around bends up to 90 degrees.[6] Studies of detonations around bends have shown detonations propagate easiest through bends with larger radii. In cases where the expansion around the inside of a corner tends to extinguish a detonation, the compressive (outside) surface of the bend creates enough wave interaction that the detonation wave is re-initiated.[7]

It has also been shown that detonations can be split and propagate into tubes 45 degrees to the initial detonation direction or 90 degrees to the initial detonation direction while still propagating in the initial direction.[6] Numerical and experimental analysis[8] of an inert shockwave propagating into a perpendicular tube shows that diffraction, or expansion, of the shock wave occurs immediately as the wave reaches the entrance of the perpendicular tube (Fig. 2). The shock wave weakens as it enters the perpendicular tube, as measured by pressures behind the shock wave. The weakest point of this transition (30% of initial pressure) is the inside corner and the strongest point (60% of initial pressure) is the outside corner where a strong reflection occurs. Additionally, the studies[8] showed a significant length of tube distance before the shock wave regained its planar structure in the branched tube.

Detonations can also propagate into larger or smaller tubes as has been shown through experiment and numerical analysis.[3,6,9,10] However, most of the cited research deals with diameter changes that are co-axial to the direction of the propagation. This current effort is fundamentally different than what has previously been done, as the detonation will be transitioning into a tube 90 degrees to the initial detonation direction and then almost immediately be required to turn 90 degrees again into the next detonation tube.

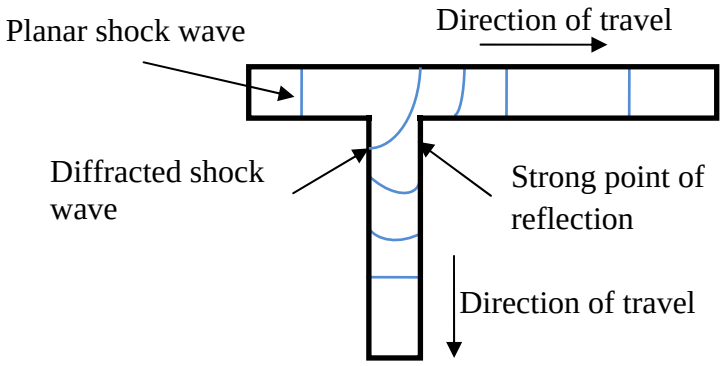


Figure 2. Inert shock wave propagating in tube perpendicular to initial propagation.

To initiate a detonation, the mechanisms of shock wave focusing and shock wave reflections have been shown to be successful. A detonation wave was experimentally shown[9] to propagate around a rectangular U-shape with help from strong reflections in the corners of the bends. This propagation was also shown[10] numerically through computational fluid dynamics, the result of which is displayed as Fig. 3. The re-transition was initiated by the strong corner reflection in the lower left corner of the figure. The successful re-transition is characterized by the regular cell structure seen in the bottom right portion of the Fig. 3.

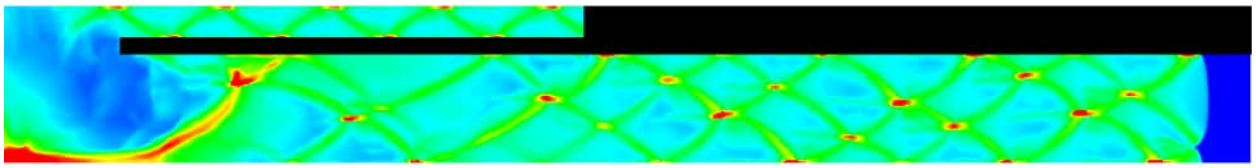

Figure 3. Numerical solution of detonation propagating around a U-shaped bend

The focusing of a shock wave has also been shown to initiate a detonation. In these experiments[11] an inert shock wave traveled down a shock tube and was then focused into parabolic, wedge and circular geometries. The shock tube was filled with a combustible mixture near the geometries. The shock wave Mach number had a large effect on the initiation of a detonation in the reflector geometries. For lower Mach numbers (< ~2.4) a strong deflagration was ignited in the reflector. Due to the compression waves emanating from combustion, this strong deflagration was capable of transitioning into a detonation after it had left the geometry. For higher Mach numbers (> ~ 2.5) a detonation was initiated in the reflector geometry and continued to propagate as it exited the geometry.

The experiments just described have shown the possibility for a detonation from one detonation tube to initiate a detonation in another detonation tube via a transverse cross-over tube. Experimentally, this tube-to-tube initiation was shown[4,5] for detonation tubes connected via a cross-over tube at the head or tail end of the detonation tubes. Due to the continuity of the detonation wave, this set-up is called a continuously operating PDE.

The setup for the continuously operating PDE (Fig. 4) employed four tubes connected tail-to-tail (e.g., tubes 1-2, 3-4) or head-to-head (tubes 2-3). All tubes are 2” in diameter. The set of tubes was connected to the PDE valving system via the flanges on the left in Fig. 4. A detonation was created by a DDT device in tube 1 and used to detonate a fresh fuel and air

charge in the successive tubes. This is an improvement over similar setups that have used unconnected tubes with a DDT device in each tube.


Figure 4. Four-tube setup successfully run on ethylene and hydrogen using tube-to-tube initiation. Arrows show direction of detonation wave.

While this continuously operating PDE concept is feasible, there is uncertainty as to what combustion physics occur in the cross-over tube. For example, it has been shown[5] that the shock wave may decouple from the combustion front through the cross-over tube and then quickly recouple. Any decoupling of the shock wave from the combustion front will cause the combustion front to decrease in velocity and possibly cause the detonation to fail. Figure 5 shows there is a loss of wave speed through the cross-over tube in relation to the main detonation tube. The cross-over tube wave speeds are 200-300 m/s less than the speed in Tube 3 and in tube 4, which both recorded detonation wave speeds consistently between 1900 and 2200 m/s.[12] The specific reason for this has not been studied. No investigation has been done to observe or optimize the travel of the detonation wave as it propagates through the cross-over tube. The current effort will visualize the detonation wave passing through a cross-over tube and

focus on determining parameters that encourage successful propagation through the cross-over tube.

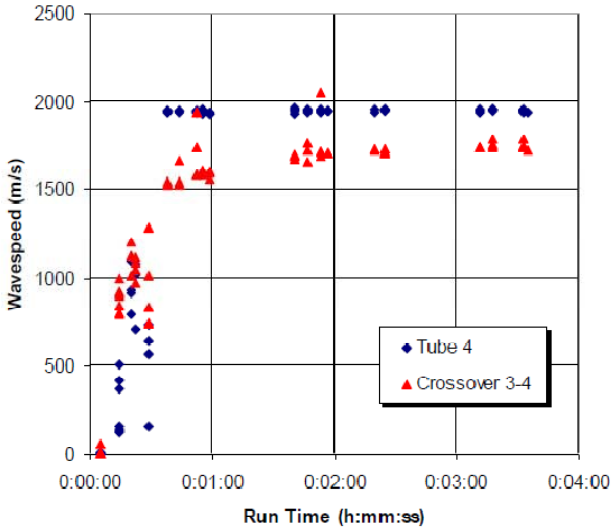


Figure 5. Wave speeds from branched, 4 tube setup as shown in Fig. 4.[12]

## 2. Detonation Wave Structure

Before a detonation event can be studied the structure of a detonation wave must be understood. A detonation in a tube can be thought of as a shock wave and combustion zone traveling, or propagating, close to one another at the speed of sound local to the shock wave, into a mixture of unburned gases. The shock wave is sustained by the energy released in the combustion zone and, in turn the combustion process is initiated by the compression from the shock wave and the resulting high temperatures just behind the shock wave.

Given a tube of sufficient length, with adequate chemical reactants and an ignition of those reactants, a detonation will form. When the mixture is ignited from the closed end, the flame front initially travels at its laminar flame speed (a deflagration), but quickly increases in speed due to the expansion of the combustion products between the flame and the closed end of

the tube. A compression wave is formed from the expansion of the combustion products and travels downstream increasing the pressure and temperature of the reactants. As the flame moves down the tube at increasing velocity, the reactants in front of the flame become turbulent. With turbulent reactants, the flame front itself becomes turbulent. This turbulent combustion zone leads to an increase in the effective flame surface, allowing it greater exposure to unburned mixture and increasing the flame velocity. This increase in flame velocity will continue until the compression waves coalesce into a shock wave and produce reactant pressures and temperatures suitable for self ignition and explosion of the mixture behind the shock wave. This shock wave is sustained by the energy released by the combustion front and the combustion process is initiated by the compression and the increased temperatures from the shock wave. [2,13] The coupled shock-wave and combustion front is termed a detonation (Fig. 6).

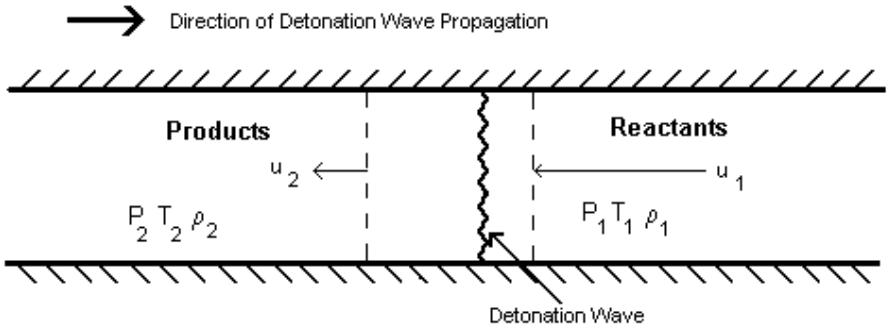


Figure 6. Detonation wave propagating in a tube.

It is important to note that there are ways of inducing turbulence into the flow ahead of the combustion wave, thus forcing an increase in the flame surface area before it would naturally occur. This method leads to the creation of a detonation in a much shorter distance. It is standard practice to introduce an obstacle into the flow to reduce the time for this deflagration to detonation transition. Spirals, ramps, or flat obstacles are often placed in the detonation tubes to 'trip' the deflagration into a detonation.

The structure of a detonation wave has been modeled by the Zeldovich-von Neumann-Doring (ZND) model. This theory is a one-dimensional representation of the complex detonation wave. The theory states that a detonation wave can be modeled in three sections, the shock wave, an induction zone and a reaction zone.[2,14] Figure 7 shows a diagram of temperature, pressure and density at various points in the detonation wave. The properties at location A are the reactant conditions and location B are the properties that correspond to the Chapman-Jouguet (CJ) point. The CJ point is the boundary between the stable reaction zone and the rarefaction wave.[13] The rarefaction wave is the expansion wave created by the expanding combustion products that follow the detonation front. The distance from A to B is on the order of one centimeter with the shock wave having a thickness on the order of the mean free path for the gas used, typically nanometers ($10^{-9}$ m). This diagram shows the necessity of keeping the shock wave and combustion front coupled. If the reaction zone lags only slightly from the shock wave, conditions will not be adequate for auto ignition of the reactants and the combustion will revert back to a deflagration.

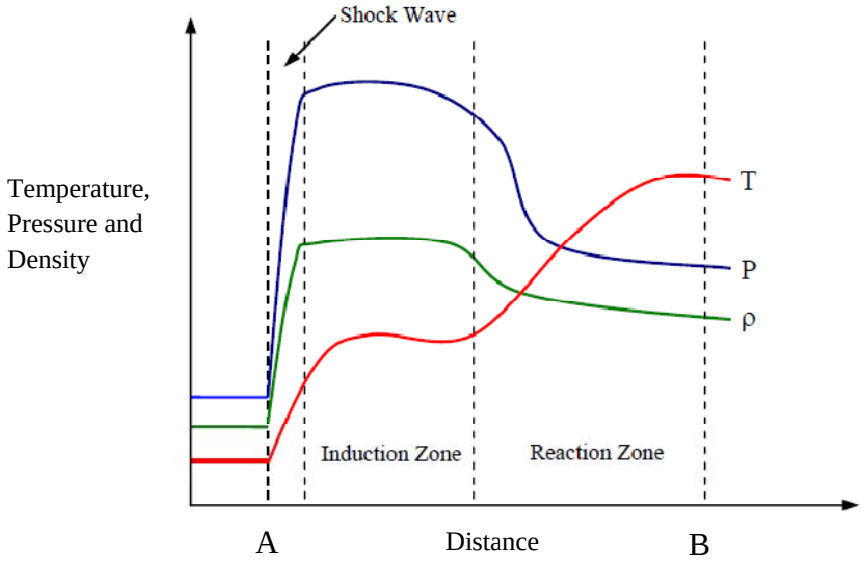


Figure 7. Pressure, temperature and density through detonation wave (not to scale)

## 3. Detonation Velocity

Though a detonation is complex, a detonation wave will propagate at a certain theoretical velocity. This wave speed is called the Chapman-Jouguet velocity ($V_{CJ}$ or CJ speed), measured at the previously mentioned Chapman-Jouguet point in the detonation wave. The CJ speed is developed through a one dimensional approach initially developed by Chapman and outlined by Stephen Turns in reference 2. This analysis starts with six assumptions:

1. One-dimensional, steady flow
2. Constant area
3. Ideal gas behavior
4. Constant and equal specific heats
5. Negligible body forces
6. Adiabatic conditions

From these assumptions the conservation of mass, momentum, and energy equations reduce to Eqs. (6),(7), and (8) respectively. The ideal gas equation is presented as Eq. (9).

$$\dot{m}'' = \rho_1 u_{x,1} = \rho_2 u_{x,2} \tag{6}$$

$$P_1 + \rho_1 u_{x,1}^2 = P_2 + \rho_2 u_{x,2}^2 \tag{7}$$

$$c_p T_1 + {u_{x,1}^2}/{2} + q = c_p T_2 + {u_{x,2}^2}/{2} \tag{8}$$

$$P = \rho R T \tag{9}$$

A solution to the continuity and momentum equations (Eqs. (6) and (7)) provides the relationship in Eq. (10) with $\nu = 1/\rho$. Using Eq. (10), a line for P versus ν can be plotted for a fixed mass flow rate. This line is called a Rayleigh line. Multiple Rayleigh lines are plotted for increasing mass flux indicated on Fig. 8. At the limits a Rayleigh line could be vertical (for infinite mass flux) or

horizontal for zero mass flux, pivoting at the point $P_1$, $\nu_1$. With these limits it can be seen that quadrants A and B will never have a Rayleigh line passing through them. Since Eq. (10) is based on the continuity and momentum equations, and both must be satisfied for a real result, we have shown there will never be a physical solution in quadrants A or B. This conclusion will lead to determining the CJ speed for a given mixture.

$$\frac{P_2 - P_1}{\nu_2 - \nu_1} = -(\dot{m}'')^2 \tag{10}$$

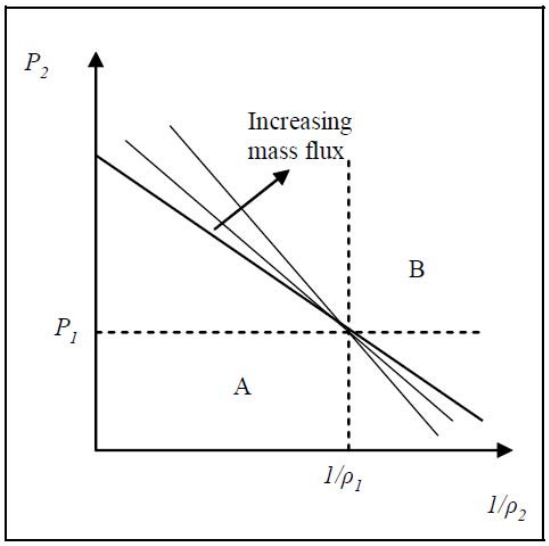


Figure 8. Rayleigh lines

$$\gamma \equiv {}^{c_p}/_{c_v} \tag{11}$$

Expanding on Eq. (10) to add the energy equation, Eq. (8), the Rankine-Hugoniot equation and curve is obtained. Through the use of the ideal gas equation and Eq. (11) the equation for the Rankine-Hugoniot curve is:

$$\frac{\gamma}{\gamma - 1}(P_2\nu_2 - P_1\nu_1) - \frac{1}{2}(P_2 - P_1)(\nu_1 + \nu_2) - q = 0 \tag{12}$$

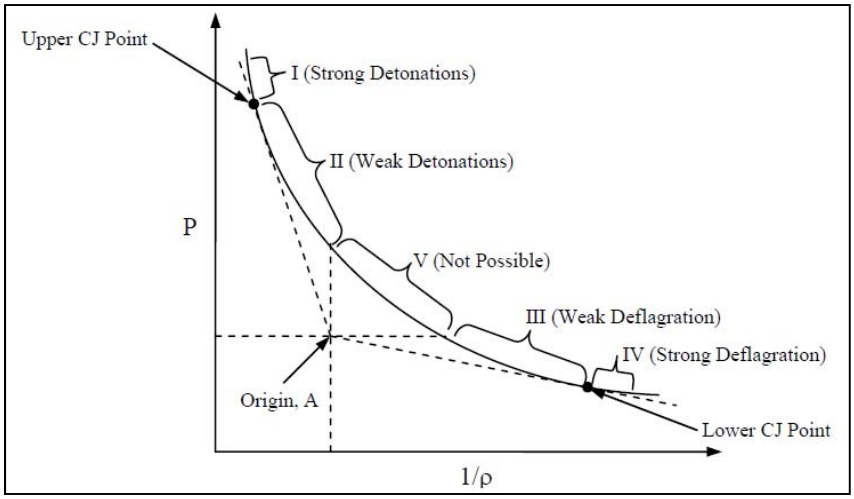


Figure 9. Rankine-Hugoniot curve (solid) with Rayleigh lines (dashed)

Figure 9 shows the Rankine-Hugoniot curve plotted with the Rayleigh line boundaries and two Rayleigh lines tangential to the curve that originate from the origin. The points of tangency are defined as the upper CJ point and lower CJ point. Knowing density, pressure and mass flux, velocity for the upper CJ point can be solved for via the Rankine-Hugoniot equation (Eq. (12)). This velocity is termed the CJ velocity and is the velocity at which a stable detonation wave propagates.

The CJ speed of a stoichiometric hydrogen and air mixture is approximately 1971 m/s and for ethylene and air the CJ speed is 1850 m/s. These speeds are specific to exact theoretical conditions and are based on the assumptions listed above. In experiment, a detonation wave can be sustained at velocities relatively far from the theoretical $V_{CJ}$, on the order of ±30%. This is due to the constant decay and re-initiation of the wave that occurs along the cell boundaries in a detonation.

## 4. Cell Size

Within the detonation front there are important wave interactions taking place transverse to the direction of propagation that sustain the detonation. Three waves: incident shock, reflected shock and Mach stem form a triple point where they meet. Wave velocity is highest at the triple point and then decays until the next triple point re-energizes the local flow. The path of triple points has been visualized by detonating through a tube that has been coated with soot. As the detonation passes the triple points erase soot from the tube wall, leaving behind what is commonly described as a fish-scale pattern (Fig. 10). The bounded areas that these triple points create are termed cells. Cell size is defined as the distance of a cell measured perpendicular to the direction of propagation and cell length is defined as the horizontal distance of a cell, measured in the direction of the wave movement. Cell size is an important parameter for determining how or if a detonation will propagate in a tube, channel or unconfined space.

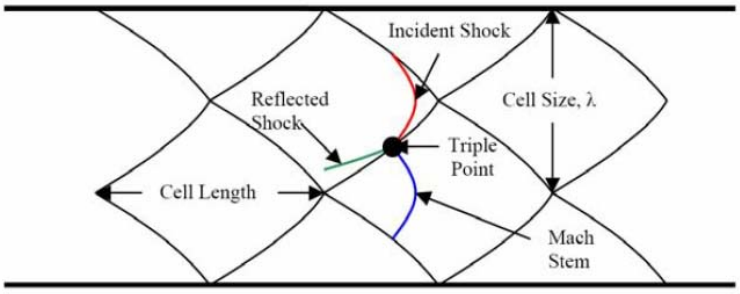


Figure 10. Internal detonation wave interaction and resulting cells

Cell size, which affects the characteristics of a detonation, is affected by the equivalence ratio (Eq. (4)) of the fuel mixture that is reacting. A graph of cell size versus equivalence ratio is shown in Fig. 11, it is clear there is a minimum for the various fuels. This occurs near an equivalence ratio of one. For the fuels used in this research, hydrogen and ethylene, the cell size is 0.7 in and 0.85 in respectively at an equivalence ratio of 1.0.

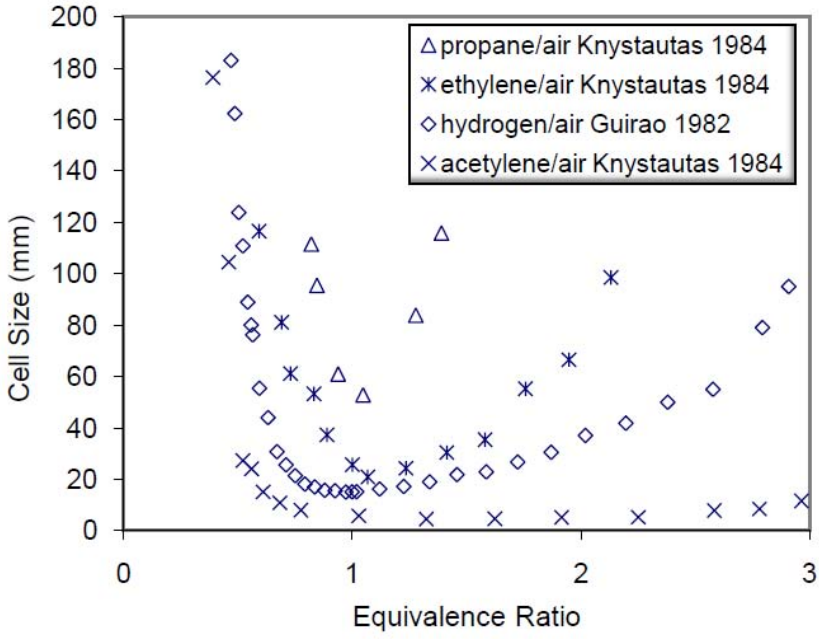


Figure 11. Cell sizes of different fuels at varying equialence ratio.[15,16]

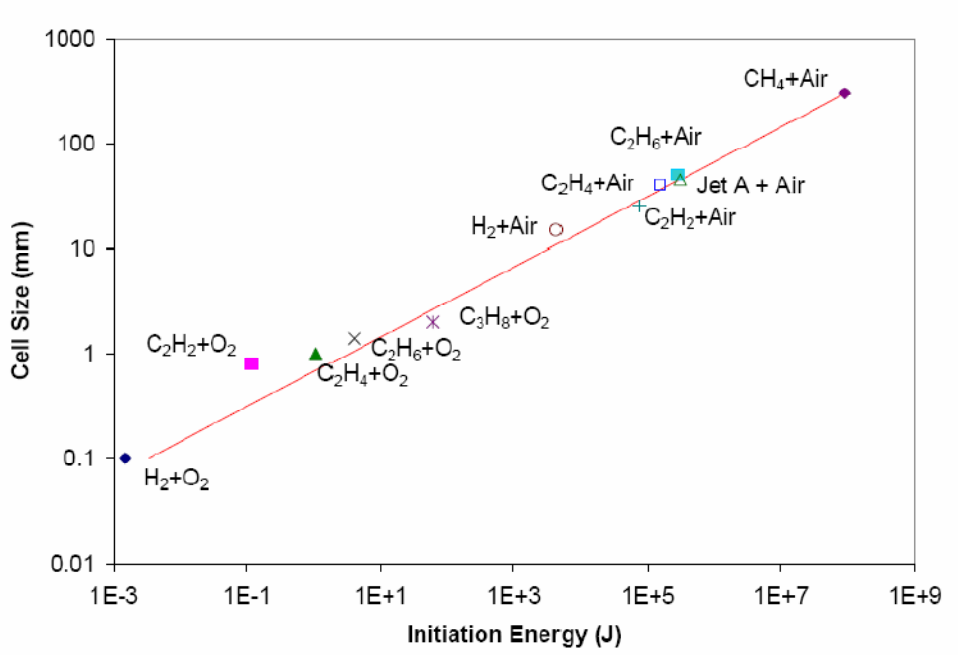


Figure 12. Cell size versus initiation energy

Cell size also has a large effect on initiation energy. Figure 12 shows the energy required to directly initiate a detonation ($E_{DID}$) versus cell size. This relationship[17] is approximated by the empirical function whose equation is given as Eq. (13). Cell size ($\lambda$) is cubed in Eq. (13), so slight variations in cell size or equivalence ratio greatly affect the initiation energy.

$$E_{DID} = 3.375\lambda^3 \tag{13}$$

When trying to initiate a detonation it is desirable to have small cell sizes so smaller amounts of energy are needed. Using oxygen as an oxidizer requires substantially less initiation energy than using air. However, flight applications for the PDE will be air breathing, so air is used as an oxidizer in this research. Hydrogen and ethylene were the fuels chosen for this research based on their low initiation energy and relative ease of detonability. An equivalence ratio near one was chosen to reduce the cell size. This choice also ensures a minimum initiation energy by Eq. (13).

**5. Detonation Propagation**

Once a detonation has been created it can take on two forms: planar or spherical. A representation of these two forms is shown in Fig. 13 from schlieren images taken during this research. A planar detonation will propagate in a confined space (i.e. a tube) and a spherical detonation will propagate in an unconfined space. There are limits on the size of the channels with respect to the success of the detonation propagation. These limits are based on cell size.

For a planar detonation to survive and propagate in a circular tube the diameter of the tube must be at least $\lambda/3$; to propagate in a square tube the height must be greater than the cell size, $\lambda$; and for a rectangular tube the height must be greater than the cell size. For a spherical

detonation that exits a round tube to survive, the diameter of the tube must be at least 13λ. For a square tube a spherical detonation will survive if the width is at least 10λ. For a rectangular tube the tube height must be greater than 3λ and the width must be greater than three times the height. These detonation limits are tabulated in Table 2. The larger tube sizes are required for spherical detonations because of the number of transverse wave interactions required for the detonation to overcome the expansion that will take place after the detonation exits the tube.[18] These limits are important as they may determine if a detonation will need to be re-initiated, or if there is enough energy for the detonation to sustain itself.

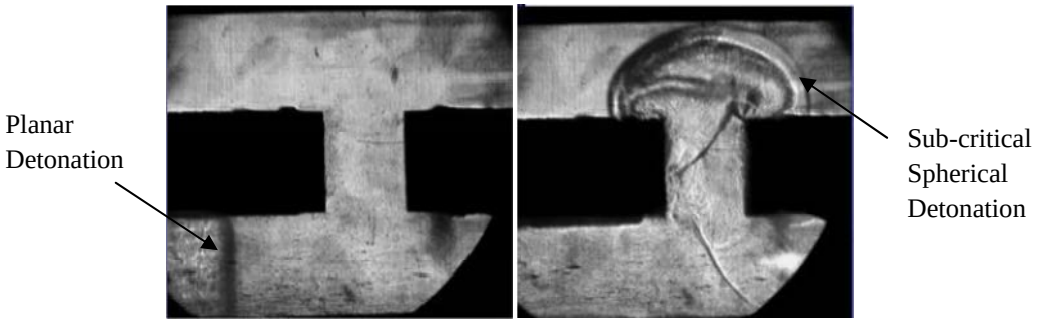


Figure 13. Representation of a planar (left) and a sub-critical spherical detonation (right). Propagation for the planar detonation is left to right in the bottom tube. Propagation for the sub-critical spherical detonation is bottom to top.

Table 2. Limits for propagation of a detonation

| | **Detonation** | |
|---|---|---|
| **Tube** | **Planar** | **Spherical** |
| Circular | $d > \lambda/3$ | $d > 13\lambda$ |
| Square | $h > \lambda$ | $h > 10\lambda$ |
| Rectangular | $h > \lambda$ | $h > 3\lambda$ and $w > 3h$ |

When a planar detonation experiences an expansion the detonation wave undergoes diffraction. Diffraction is the process of a planar detonation taking on the shape of a spherical detonation. Diffraction will occur when the detonation front is allowed to expand, such as in the

entrance to a cross-over tube or into an unconfined space as shown in Fig. 14. There are three degrees of diffraction: supercritical, near critical or sub-critical. For supercritical diffractions the detonation wave remains coupled throughout the expansion. Near critical diffractions are characterized by a detonation wave that decouples but quickly re-couples to reform the detonation wave. Sub-critical diffractions decouple into a distinct combustion front and shock wave and revert to a deflagration. Sub-critical diffractions do not, by themselves, re-transition.[19]

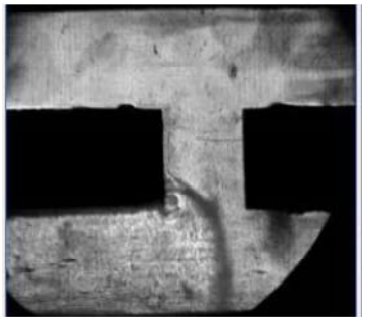

Figure 14. Diffraction of a detonation wave. Propagation is left to right in the bottom tube.

A detonation is a unique phenomenon as the shock wave and combustion front rely on one another but react as two different media. The shock wave abides by wave theory, whereas the combustion front will behave more like a continuous fluid as it will follow the bulk motion of the reactants. This is especially important to note as this research focuses on turning a detonation. As the detonation is redirected, both the shock wave and combustion wave will behave differently.

**6. Detonation Visualization**

To visualize the detonation event a schlieren technique is used. This is a common laboratory visualization technique using the property that light diffracts through media of varying density. The schlieren method is a popular technique because of its relative ease of setup and

high quality of images.[20] The schlieren setup consists of a concentrated light source, a converging mirror to collimate the light and a collecting mirror which collects the light after it has passed through the region of interest. Between the converging and collecting mirrors additional flat mirrors may be used if the light train needs to be redirected. As the collimated light beam passes through a fluid in which the density (and therefore refractive index) varies it will be deflected. After the light beam reflects off of the collecting lens, the deflected and undeflected light rays have different focal points. A knife edge is used to block the deflected rays at the focal point of the un-deflected rays, allowing the un-deflected rays to pass through to the camera. When viewing an schlieren image, dark spots are interpreted as locations of high density gradient (more deflection) and light regions of less density gradient (less deflection). A schematic of the schlieren set-up used for this research is presented in the next section.

## III. Test Setup

### 1. Facility

All research was conducted at the Detonation Engine Research Facility (DERF) at Wright Patterson Air Force Base, Ohio. The PDE program is under the Air Force Research Laboratory, Propulsion Directorate, Turbine Engine Division, Combustion Branch (AFRL/RZTC). The DERF houses an indoor, large engine test facility originally configured to test turbojet engines generating up to 60,000 lbf of thrust. It has since been converted for detonation engine research. The conversions include a thrust stand and systems to regulate air and fuel flow to the PDE.

The base component of the PDE is the cylinder head of a GM Quad 4 engine (Fig.15). The cylinder head has four valves for each detonation tube, two for the fill mixture and two for the purge air. The valves are operated by a camshaft that is driven by an electric motor, located directly behind the PDE head in Fig. 15. Pressurized air is fed to the PDE by a compressor capable of supplying 1412 $ft^3$/min of air at 100 psi. The air separates into two streams for the fill and purge and is controlled by choked nozzles and pressure regulators. The required air mass flow, and therefore nozzle diameter, is determined by total tube volume and cycle frequency. Fuel is also supplied to the engine through pressurized tanks and nozzles. The amount of fuel mixing with the fill airstream is set by tank pressure and sonic nozzles with known throat diameters. Spark plugs in the stock cylinder head location are used to ignite the mixture. The detonation tubes are bolted directly to the cylinder head and one to four tubes can be used at a time.

The PDE is controlled by an operator from a control room adjacent to the test cell. Control software monitors all of the mechanical systems that operate the PDE. The software

allows the operator to adjust many operating parameters to include equivalence ratio, fill and purge fractions, ignition delay, number of sparks, and engine speed for each run.

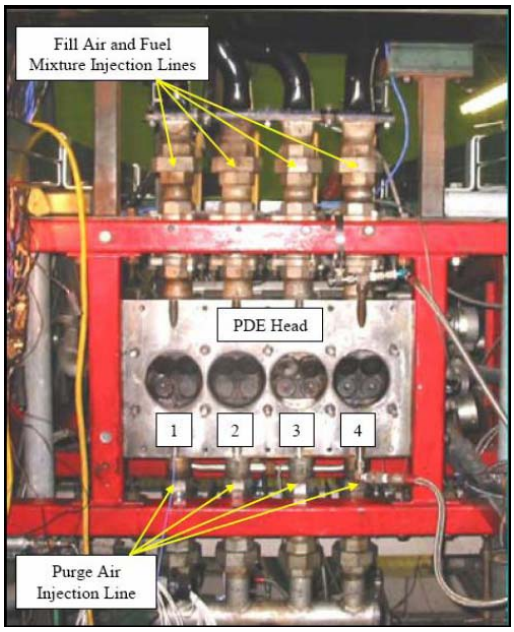


Figure 15. Research PDE head

**2. Test Section**

To study the propagation of a detonation through a cross-over tube, a test section which allowed for visualization, varying cross-over widths and varying cross-over geometries was fabricated. The test section is made up of four main parts: the base, adjustable center box, clear polycarbonate panels and metal 'cages' (Figs. 16 – 18). The base (Fig. 16) provided the internal structure for the test section tubes. The base also provided the mounting surface for the test section to connect to tubes coming from the PDE head. All individual elements of the base were welded together. The welding operations were performed on outer surfaces to ensure smooth tube walls in the test section. Figure 17 is a drawing of the adjustable center box that was mounted in the base structure. The slotted holes allowed for the center box to be moved forward

or backward up to 1” while installed in the test section, thereby increasing or decreasing the width of the cross-over tube. Both the adjustable center box and the base have four threaded holes on the flat surface that makes up the cross-over tube. These attachment points allowed for a 1” standoff block to be added, thus allowing total adjustments of up to 2” in cross-over tube width. Additionally, they provided the mounting points for the various geometries that were added to the cross-over section. The cage and polycarbonate (Fig. 18) allowed for three distinct viewing locations, while providing adequate support for the polycarbonate and adequate clamping force to seal the test section. The viewing locations are the middle cross-over section and the sections to the left and right of it. The seal between the polycarbonate and the test section was made with the use of high temperature RTV. A seal was required to ensure there was no leakage between the tubes of the test section or from the test section to the test facility.

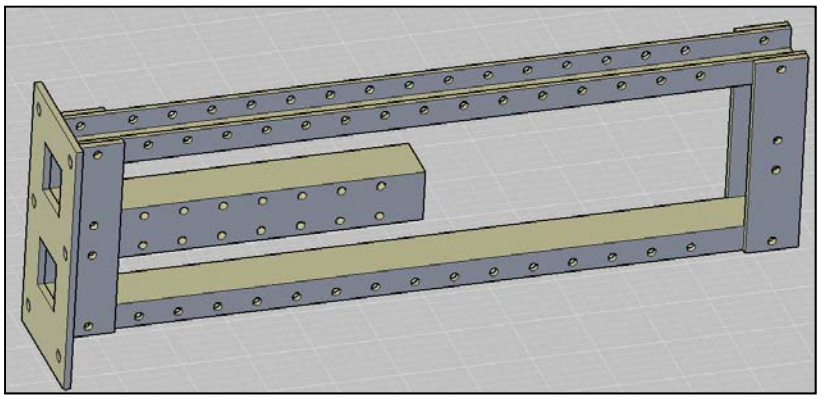

Figure 16. Test section base structure

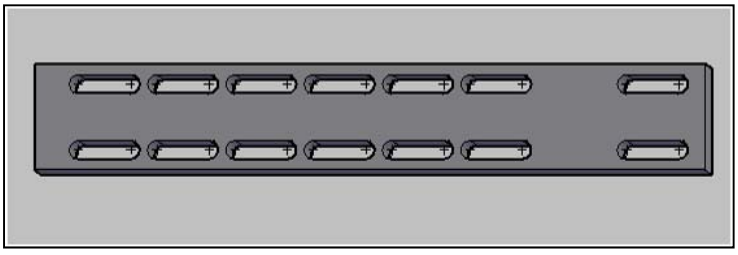

Figure 17. Adjustable center box that allows for variable cross-over width.

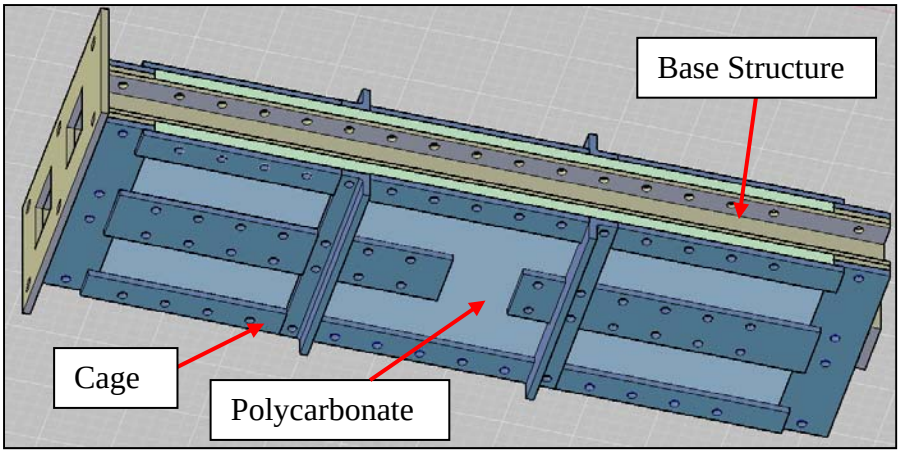


Figure 18. CAD drawing of fully assembled test section

When assembled (Figs. 18 & 19), the test section formed 2” by 2” square tubes that were 28” in length. This is similar to the continuously operating PDE[5] (Fig. 4) that used round tubes with a 2” diameter. The square-to-rectangular cross-over section is located in the middle of the test section and is adjustable from 0”-2” in the x-direction (width) as indicated in Fig. 19. The cross-over is fixed at 2” in the y and z directions (height and depth). The 0.5” thick clear polycarbonate was thick enough to resist cracking but still allow for the desired visualization. The bolt spacing that held the outer cages on was used based on prior experience and verified by a beam bending calculation. The test section mounted to round detonation tubes from the PDE head via the flange to the left in Fig. 18.

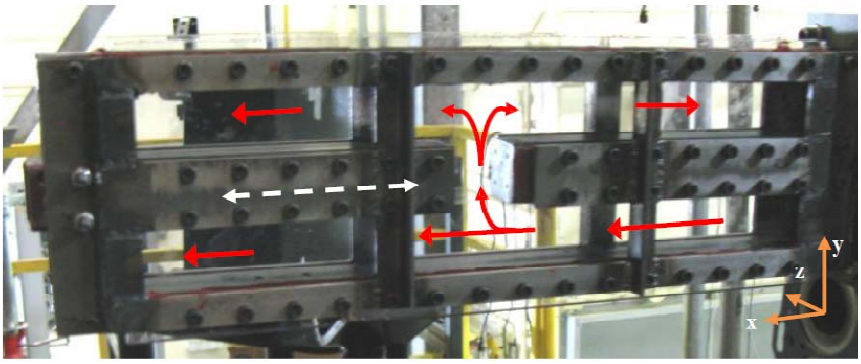


Figure 19. Test section with adjustable cross-over section. Red arrows indicate direction of detonation. White, dashed arrow indicates moveable portion of the test section.

## 3. Test Series Configurations

This effort was divided into three broad test series, each of which used the test section just described. Each test series was unique in its own way and expanded on the one previous to it. The goal for the 1st test series was to visualize the detonation through the cross-over tube and find limits for the width of cross-over tube that allowed a detonation to transition from tube 4 to tube 2.

Two tubes, each 48" in length and 2" in diameter were mounted to cylinders 2 and 4 of the PDE head (Fig. 20). Downstream of these tubes was an adapter to turn the tubes from a horizontal orientation to a vertical orientation (Figs. 20 & 21), for easier viewing via schlieren optics. The test section was bolted to the adapter. The adapter utilized head gaskets from the PDE head on each mounting surface to ensure a gas tight seal and to account for any minor misalignments.

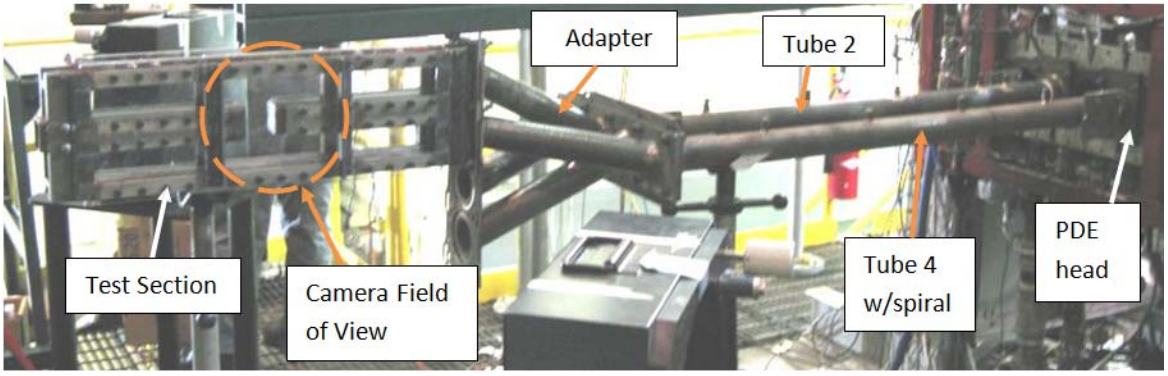


Figure 20. Test setup from PDE head to test section

For the operation of this setup a detonation is created in tube 4 via DDT. A 36" shchelkin-like spiral is used in tube 4 to accelerate DDT. Its length was chosen based on the anticipated fuels being used (hydrogen ($H_2$), ethylene ($C_2H_4$)). A standard automotive spark plug in cylinder 4 initiated the deflagration. Once DDT occurs, the detonation will travel downstream

in tube 4, through the adapter and enter the bottom tube of the test section, which will be referred to as tube 4. The detonation will then travel into the cross-over tube and continue upstream in tube 2, towards the PDE head. For the 1st test series a rectangular cross-over tube (Figs. 19 & 20) was used. The detonation's path of travel is shown schematically as the red arrows in Fig. 19.

For the remainder of this document the term 'upstream' will refer to the direction towards the PDE head and 'downstream' will refer to a direction away from the PDE head. This convention is used based on the fill and purge flow directions, not the detonation direction.

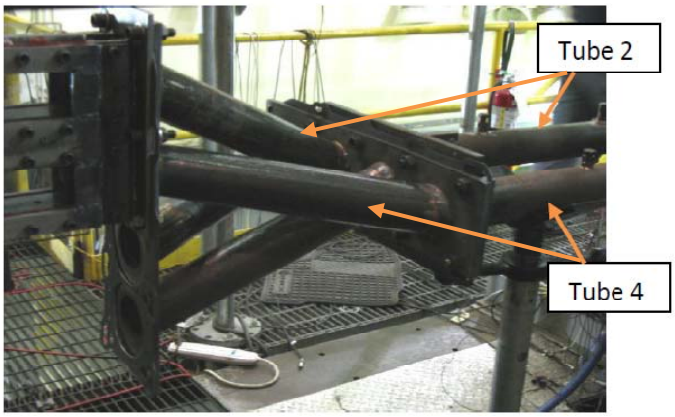


Figure 21. Adapter used to rotate test section for improved visualization.

A stock camshaft from the General Motors engine was used for the 1st test series. The stock camshaft lobes are 90 degrees apart (Table 3) and the engine firing order is 1-3-4-2 (Fig. 15), so tubes 2 and 4 are 90 degrees apart in activation. This offset in timing resulted in an undesirable flow interaction between tubes 2 and 4 via the cross-over tube and will be discussed further in the results section.

The 2nd test series aimed at fixing the timing issues found in the 1st test series and to determine if different cross-over geometries affected the propagation of the detonation into tube 2. The PDE setup was the same as the first test series, except the second test series utilized a

custom camshaft (Fig. 22) with timing as labeled in Table 3. With this timing there was less interaction between tubes 2 and 4 as desired. However there was an issue with an air-spring pulling pure air into the test section and leaning out the mixture in the test section, this issue is explained fully in the results section.

Table 3. Camshaft lobe design angles

| | Lag Angle (Degrees Rounded Down) | |
|---|---|---|
| Cylinder | Stock Cam | Custom Cam |
| 1 | 0 | 0 |
| 2 | 270 | 14 |
| 3 | 90 | 14 |
| 4 | 180 | 18 |

Figure 22. Custom camshaft used for test series two.

The cross-over shape was varied for the 2nd test series. A rectangular cross-over along with three additional cross-over geometries were used. Curved geometries (Figs. 23 & 24) were used in the cross-over tube to determine if they helped promote propagation. Geometry "S" was designed to ease the transition of the detonation wave into and out of the cross-over tube, as opposed to the sharp corners and the immediate volume change the detonation wave encounters with the rectangular geometry. Geometry "U" was designed to utilize findings[7] that a curved surface will help to produce multiple wave reflections and re-initiate a detonation on the outer radius.

Finally, the U shaped geometry was modified to encourage transition of the detonation to tube 2. Small bumps were placed on the inside of the cross-over tube, along with a plate at the exit of the cross over that was angled into the cross-over tube. A cartoon of the geometry is shown in Fig. 24. The goal of these modifications was to slow the shock wave and combustion front on the inside of the cross-over tube so it did not travel into tube 2 and start reacting with the mixture before the higher energy waves on the outside of the cross-over made it into tube 2.

With the geometries attached, the adjustable cross-over was limited to a range of 0.0" to 1.7" in width.

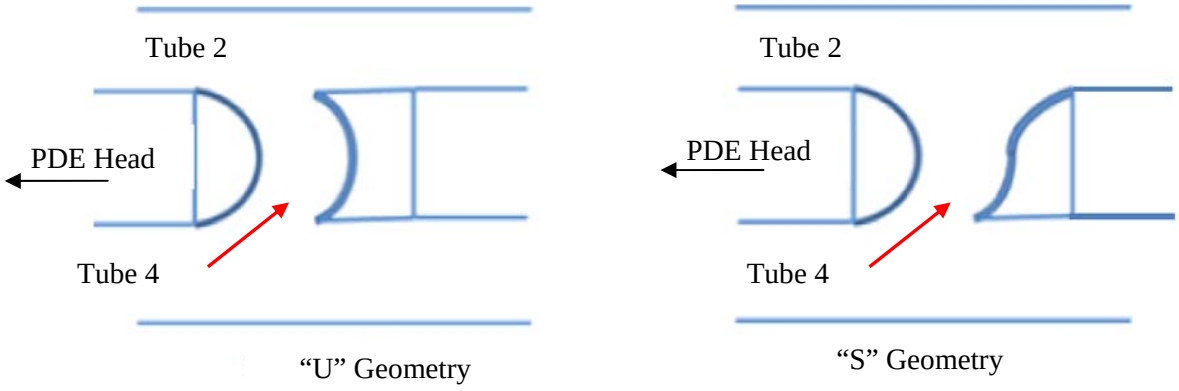


Figure 23. Cross-over geometry for test series two. Red arrow indicates direction of detonation into cross-over

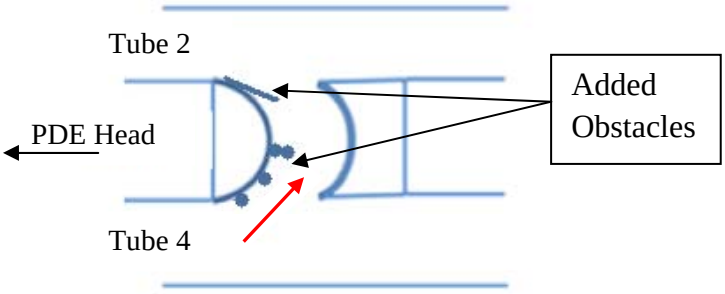


Figure 24. Modified "U" geometry with additional obstacles. Red arrow indicates direction of detonation into cross-over.

The goal of the 3rd and final test series was to re-initiate a detonation as quickly as possible in tube 2, since all previous test series observed the shock wave and combustion front decouple into and out of the cross-over tube. The 3rd test series used a slightly different setup than the first two series. Instead of the two tube setup described previously, only one tube from the PDE head was used (Fig. 25), as it was desired only to see what was happening in the test section, not farther upstream in tube 2. A nozzle was mounted to the end of the test section on tube 4 to help force flow into tube 2 (Fig. 26). Tube 2 is open to atmosphere at both ends. The stock camshaft was used for this series as there are no timing issues with only one tube active. In this setup the air-spring was not an issue.

The "U" shaped geometry was chosen to be used in the cross-over tube based on the favorable wave speeds and reflections it produced in the 2nd test series. Due to the different PDE setup, a baseline run was completed with the "U" shaped geometry. After the baseline run, 3/8" tall static mixers, or obstacles, that spanned the full depth of the test section were added in the cross over tube and on the upper and lower walls of tube 2, immediately upstream of the exit of the cross-over tube (Fig. 27). The purpose of these obstacles was to create locations for re-initiation of the detonation as soon as possible after the exit of the cross-over tube. The obstacle in the cross-over tube and the first obstacle on the ceiling of tube 2 have small gaps, 3/16" tall , as depicted in Fig. 28, which allow for the waves and gases to pass between the obstacle and the tube wall. With gases propagating on both sides of the obstacle a backside of the obstacle may become a re-initiation surface as was shown by Lieutenant Fievesohn in Ref. 9. The additional obstacle on the top of tube 2 and the three obstacles on the bottom of tube 2 had no gaps.

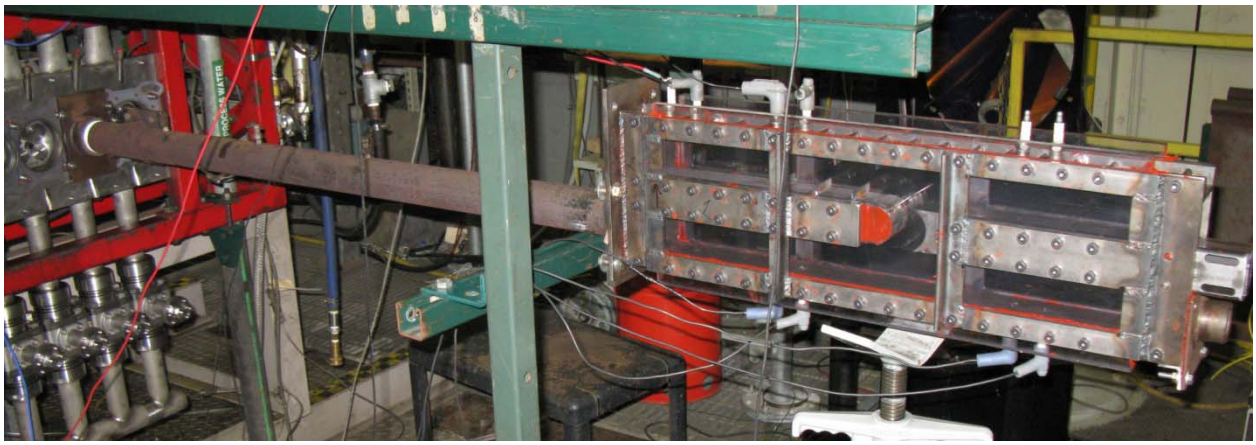

Figure 25. Test series three setup, only one detonation tube used.

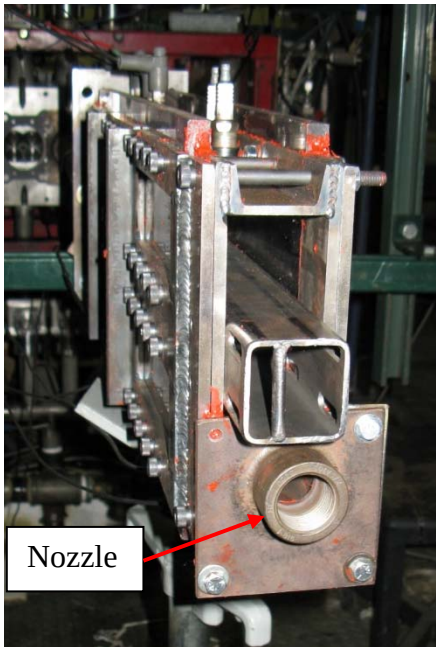


Figure 26. Nozzle for test series three, 1" nozzle shown.

An additional technique that was used for the third test series was to turn off the light source for the schlieren photography and let only the illumination from the flame front be recorded by the camera. This technique helped to determine where the combustion reaction was taking place.

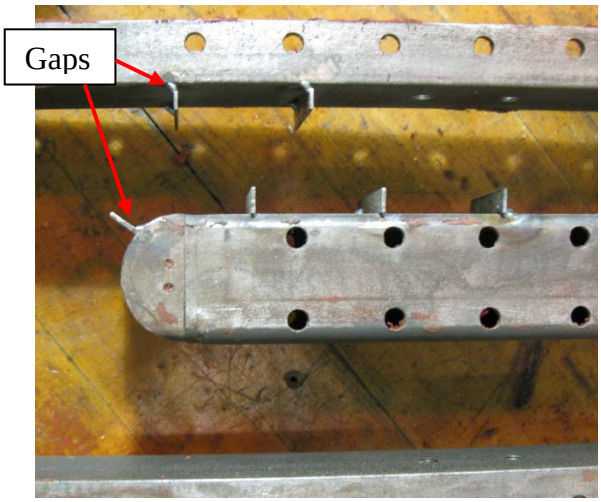


Figure 27. Six obstacles added for test series three, two obstacles contained gaps between the obstacle and test section wall.


Figure 28. Cartoon of obstacle structure for cross-over obstacle and leading obstacle on the top of Tube 2.

The engine was operated at 10 Hz in all test series. This equates to a phase duration of 33 ms for each phase (fire, fill, purge), a full PDE cycle is accomplished in 0.1 seconds. Each test run consisted of five successive detonation events (0.5 second duration).

## 4. Schlieren Setup

Schlieren photography was used to record the changes in density in the test section during a run. The setup included two spherical mirrors, 10” in diameter with a focal length of 100 inches and two flat mirrors 12.5” in diameter to direct the collimated light through the test section (Fig. 29). To record the detonation events a Phantom 7.1 camera was used. A resolution of 256 x 256 was chosen to achieve a frame rate of 26,315 frames per second. At this resolution

and frame rate the camera was capable of a 2 μs exposure time with 37 μs between exposures. These chosen parameters allowed for a field of view of approximately 8x8 inches, shown in Fig. 20. Four of the five consecutive detonation events were able to be captured with the memory available on the camera for the 1st and 2nd test series at the chosen frame rate. Due to the slightly different engine setup in the third test series, the camera was able to capture all five detonation events.

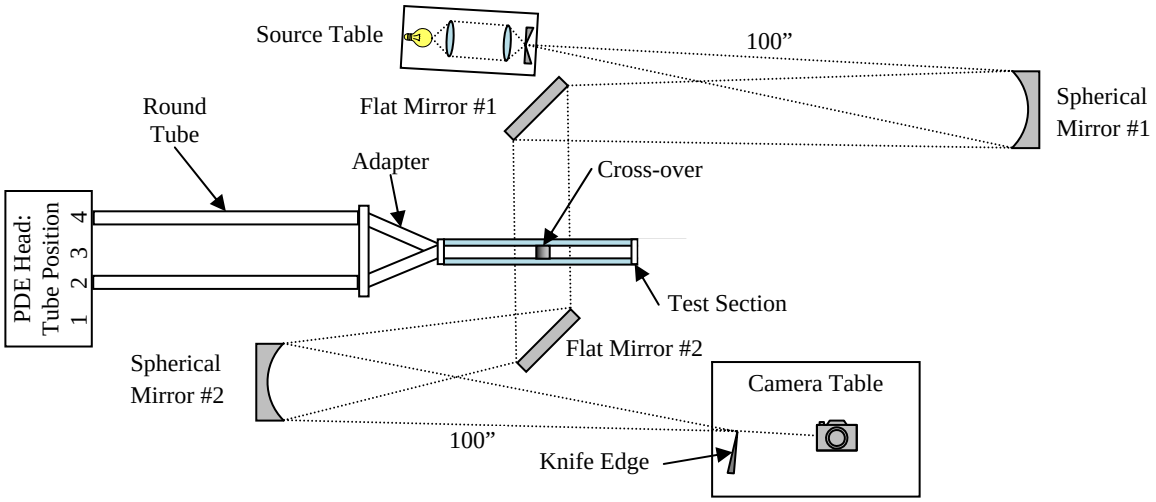


Figure 29. Schlieren set-up for all test series[21]. PDE setup shown is for the first and second test series. Flat mirrors were movable to view different locations in the test section.

## 5. Instrumentation

Since $V_{CJ}$ is a consistent indicator of a successful detonation combustion wave speeds were measured with ion probes and the schlieren photographs. Ion probe pairs were used to measure average wave speeds at four locations in the test section and one location upstream of the test section. The schlieren photographs were used to measure average wave speeds at four locations in the test section. It is important to note that the combustion wave was the feature measured with both the ion probes and the wave speeds calculated from the photographs.

The ion probes are motorcycle spark plugs. A differential of 10 volts is placed across the ion probes and as the combustion front passes, the gas ions complete the electrical circuit and cause a momentary drop in voltage. By placing two probes at a known spacing and measuring the time between voltage drops, average velocity is calculated. Four pairs were in the test section and are shown in Fig. 30 and one pair was upstream in tube 2, 30" and 40" from the PDE head.

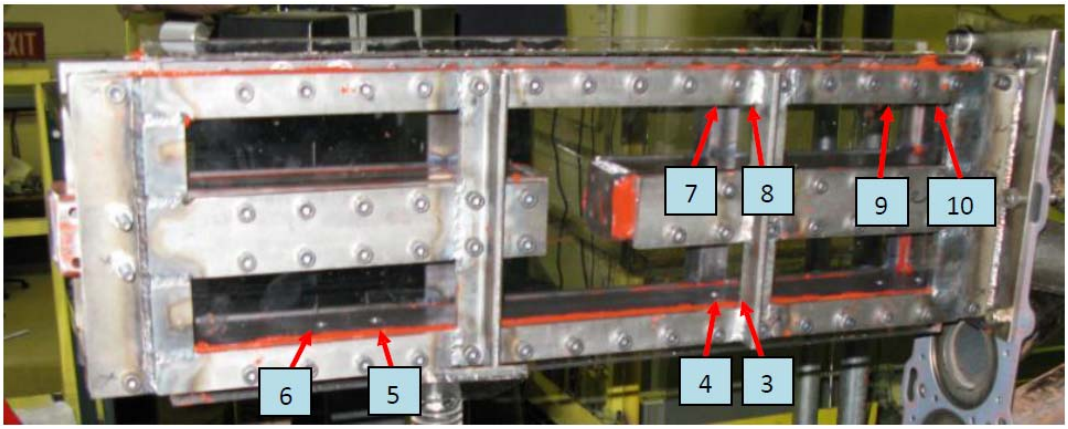


Figure 30. Ion probe numbers and locations in the test section, spacing is 1.5" between probes in the test section. One additional pair (probes 1 & 2) was located on tube 2, 30" and 40" from the PDE head.

To calculate wave speed from the schlieren photographs the 2" distance between the tubes was related to the pixel count of the same distance in the photograph. The relationship was calculated to be 38.5 pixels per inch. Two consecutive images were studied to determine the distance a combustion wave moved between the two exposures. With the time between exposures known (37 μs), the distance per pixel known and the pixel distance a gas event moved from one frame to the next known, velocity can be easily calculated:

$$Velocity = \frac{\left(meters/_{pixel}\right) x(pixels\ moved)}{time} \tag{14}$$

Average wave speeds were calculated via the photographs at locations depicted in Fig. 31.

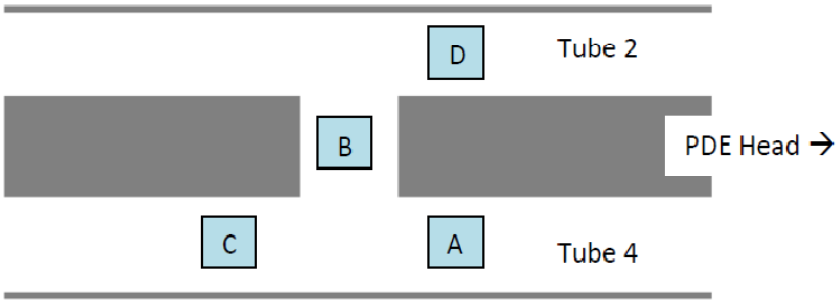


Figure 31. Location of wave speeds calculated with schlieren photographs.

Because of the distance moved between frames (1" – 2") and the smear caused by the 2 μs exposure it was not attempted to track an individual particle of the combustion front in the schlieren photographs. Instead, the measurement was always made on the centerline of the tube at the best approximation of the leading edge of the combustion front. This leads to a slightly conservative measurement as the waves do not move solely in the x direction.

## 6. Uncertainty

An uncertainty analysis was conducted for the average wave speed measurements taken from the ion probes and the schlieren photographs. The procedure for this analysis was taken from Tavoularis[20] and is based on bias and precision uncertainty. Bias uncertainty includes the fixed or constant error in each measurement system, and precision uncertainty is the random error component, sometimes called repeatability error. The bias uncertainty (B) of each measured variable was calculated as the root sum of squares of the estimated error sources with Eq. 15. The precision uncertainty (P) of each measured variable was calculated from the standard deviation (σ) of a series of measurements where available by Eq. 16. The total uncertainty, Eq. 17, is the root sum of squares of the bias and precision errors.

$$B = \sqrt{\sum_{k=1}^{k} B_k^2} \tag{15}$$

$$P = 2\sigma \tag{16}$$

$$U = \sqrt{B^2 - P^2} \tag{17}$$

For the wave speeds measured with the ion probes there were two sources of uncertainty: the actual distance between the probes and the actual time of arrival of the combustion front at the ion probe. The ports for the probes were drilled on a mill with a digital readout accurate to ±0.0005 inches. The spacing uncertainty is therefore 0.00025 inches. The arrival time bias uncertainty for the ion probes was calculated by Lt Col Hopper in Ref. 5 and is 0.502 μs. This takes into account the time uncertainty in the data acquisition system (±0.5 μs at 1MHz sampling rate) and the response time of the ion probes themselves (±0.5 μs).

The precision uncertainty of the ion probe calculations is a function of the three dimensional effects in the detonation wave. Based on differences in arrival time at an ion probe for detonation waves traveling consistently at $V_{CJ}$ the precision error is found to be 2.4 μs.[5] There is no additional precision error based on spacing as the ion probes are fixed in place and do not move.

Table 4. Wave speed measurement uncertainty for ion probes

| Spacing, Δx (in) | Bias Uncertainty, $B_{WS}$ (m/s) | Precision Uncertainty, $P_{WS}$ (m/s) | Total Uncertainty, $U_{WS}$ (m/s) |
|---|---|---|---|
| 1.5 | 50.98 | 244.71 | 249.97 |
| 10 | 7.65 | 36.71 | 37.50 |

The total uncertainties for the ion probe wave speed calculations are reported in Table 4. These uncertainties are based on a hydrogen and air mixture traveling at $V_{CJ}$ = 1971 m/s. Due to the large error for the 1.5 inch spacing, these wave speeds were used cautiously and only when repeatability in the numbers was observed.

The uncertainty of the average wave speeds calculated via the schlieren images was determined in the same way as for the ion probes. The uncertainties were again based off of a detonation of hydrogen and air moving at a speed of 1971 m/s (117 pixels moved) and also at 1000 m/s (60 pixels moved) as these were common wave speeds seen in the test section.

The bias uncertainty was based on the difficulty of determining where the leading edge of the combustion front was in the schlieren image, this led to an uncertainty of 1 pixel in the image. The time between frames was also a source of uncertainty, but was accurate to within 2 μs, giving an uncertainty of 1 μs.

The precision error was based on the differences in reported time between frames. Upon study of 25 successive frames the average was 38.25 μs with a standard deviation of .44 μs. This leads to an uncertainty of .88 μs. The random human error in picking pixels on the images has an uncertainty of 0.5 pixels. With these values, the uncertainty for the wave speeds calculated by the schlieren images are reported in Table 5.

Table 5. Wave speed measurement uncertainty for schlieren image calcualtions

| Spacing, Δx (pixels) | Bias Uncertainty, $B_{WS\ (m/s)}$ | Precision Uncertainty, $P_{WS\ (m/s)}$ | Total Uncertainty, $U_{WS}$ (m/s) |
|---|---|---|---|
| 117 | 53.49 | 44.95 | 69.88 |
| 60 | 31.04 | 24.17 | 39.34 |

The schlieren pictures are only two dimensional and no information is available for the third dimension (z-direction in Fig. 19). If the combustion wave front was not parallel with the y-z plane this could lead to an error in the wave speed calculations via the pictures. It is very difficult from the pictures to quantify any misalignment in the y-z plane. However, based on a calculated wave speed, the amount of smear can be calculated in the exposure time. A shock wave was measured to be 2 pixels in length, when traveling at a calculated wave speed of 740 m/s. For this wave speed the smear is 2.13 pixels, meaning the shock wave has virtually no thickness. This is what we would expect. If there were any significant three dimensional effects the shock wave would appear quite thick. Additionally, there is no reason to expect three dimensional effects as both walls of the test section were prepared in the same way and the geometries were made to keep the cross-over width as constant as possible. Finally only an average wave speed is desired, so even if the combustion front does vary in the z direction, measuring the front of the wave, which is visible via the schlieren photographs will give the average velocity for the wave across the measured distance. For these reasons 3-D effects will be assumed negligible.

# IV. Results

## 1. Test Series 1

The 1st test series was run with the stock camshaft and a purge fraction of 1.0 for all runs, the test parameters and results are shown in Table 6. The wave speeds in Table 6 were calculated from the schlieren images and are an average of the four successive detonation events recorded by the camera. It is evident that all wave speeds coming into the test section were 15% - 45% less than the CJ speed for a detonation. Runs one and three were the closest to CJ speed with a spark delay of 0.0 ms.

Table 6. Incoming wave speeds for first test series.

| Run | Cross over width (in) | Fuel | Fill Fraction | Equivalence Ratio | Spark Delay (ms) | Wave Speed* (m/s); loc. A (Fig. 31) |
|---|---|---|---|---|---|---|
| 1 | 2 | $H_2$ | 1.1 | 1.1 | 0.0 | 1655 |
| 2 | 2 | $H_2$ | 1.1 | 1.1 | 5 | 1118 |
| 3 | 2 | $H_2$ | 1.2 | 1.1 | 0.0 | 1681 |
| 4 | 2 | $H_2$ | 1.1 | 1.1 | 24.75 | 1285 |
| 5 | 2 | $H_2$ | 1.1 | 1.1 | 27 | 1149 |
| 6 | 1.35 | $H_2$ | 1.1 | 1.1 | 27 | 1237 |
| 7 | 1.35 | $H_2$ | 1.2 | 1.1 | 27 | 1206 |
| 8 | 1.35 | $H_2$ | 1.2 | 1.2 | 27 | 1074 |
| 9 | 1 | $H_2$ | 1.1 | 1.1 | 27 | 1351 |
| 10 | 2 | $C_2H_4$ | 1.1 | 1.1 | 20 | 1526 |
| 11 | 2 | $C_2H_4$ | 1.1 | 1.4 | 25 | 1490 |
| 12 | 1.35 | $C_2H_4$ | 1.1 | 1.1 | 25 | 1307 |

*($V_{CJ}$ for Hydrogen = 1971 m/s, Ethylene = 1850 m/s)

The 90 degree camshaft offset between the two cylinders allows for only an ~8 ms overlap in phases for Tubes 2 and 4. A graph of the timing is shown in Fig. 32. For runs 1-3, with a 0.0 ms or 5.0 ms delay, tube 2 had not finished its fill phase when tube 4 was igniting the

fuel and air mixture. With no fuel and air mixture in tube 2, there was no chance of initiation. To ensure tube 2 has had adequate time to completely fill, runs four to twelve waited until the end of tube 4's fire phase to send the spark signal to the spark plug. Neither the spark delay change nor the perturbations in the other variables provided the conditions for CJ speed.

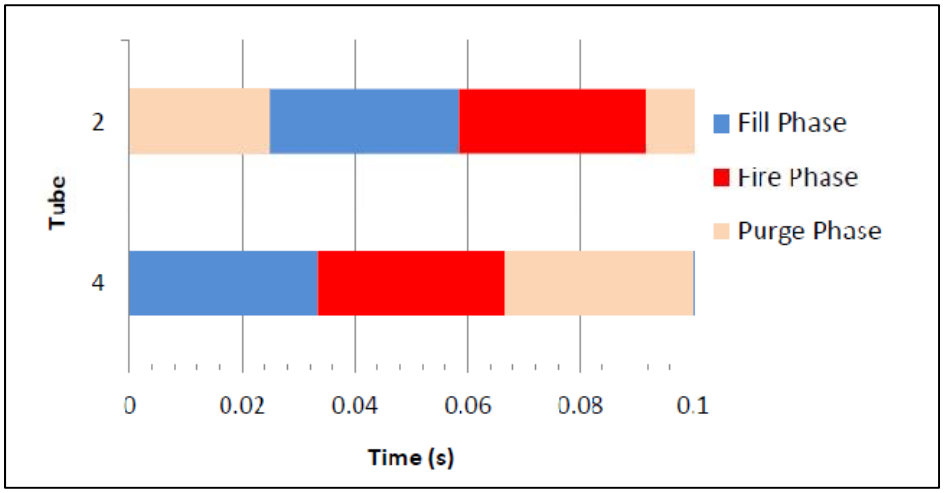


Figure 32. PDE phase offset for tubes 2 and 4 with stock camshaft. Approximately 8 ms overlap in each phase

The large spark delay in runs 4-12 created the opportunity for an undesirable interaction between the tubes. At the end of tube 2's purge phase, it was filled with pure air and tube 4 was nearly completely filled with mixture at the desired equivalence ratio. This is shown as a cartoon in Fig. 33. The beige represents pure air and the blue represents a fuel and air mixture. When tube 2 starts the fill phase the volume of pure air from tube 2 is pushed out the end of the test section and also into tube 4. This leans out the mixture in tube 4 to one that is insufficient to support detonation, hence the low wave speeds measured coming into the test section (Table 6). This finding also supports the higher wave speeds seen in runs 1 and 3, as the fill phase from tube 2 had not yet affected tube 4.

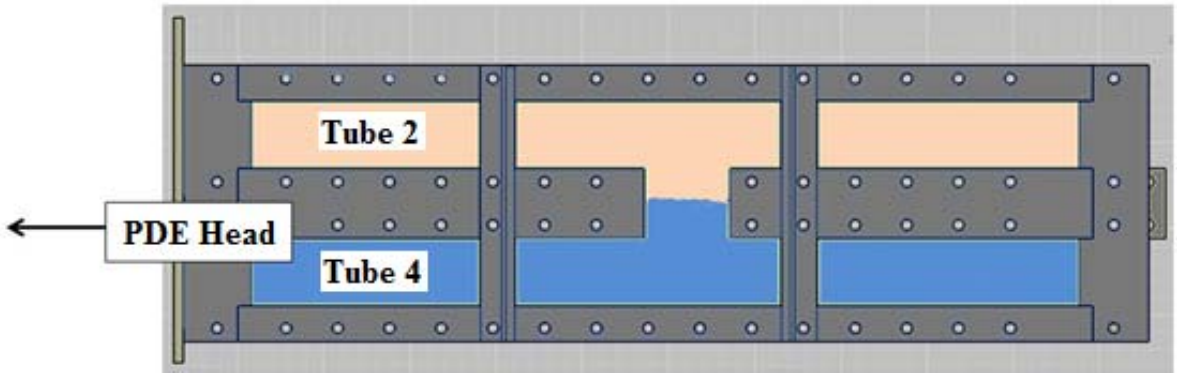


Figure 33. Cartoon of gas state at end of tube 2's purge phase with stock camshaft. Blue represents fresh fuel/air mixture, beige represents pure air.

The first test series was not able to achieve CJ wave speeds into the cross-over tube because of the PDE timing. However an important result was reached: in previous operation, detonation tubes were isolated from one another, now that they have been connected it will be essential to take note of the effect they have on one another.

**2. Test Series 2**

To rectify the timing issue discovered in the first test series the PDE head was changed to a head with the custom camshaft (Fig. 22) installed. The custom camshaft provided the timing diagram shown in Fig. 34. This change eliminated interaction between the tubes as the phases for Tubes 4 and 2 were offset by only 4 degrees of camshaft rotation, the two tubes' phases overlapped by 31.9 ms.

The setup in the 2$^{nd}$ test series provided better results than the 1$^{st}$ test series, but there were still equivalence ratio issues due to the presence of an air-spring. When the fill valves open, the fill mixture flows down the detonation tubes and out the open end. When the fill valves close the mixture that has just entered the tube is still flowing towards the open end. This

creates a low pressure region near the PDE head, enough that flow reverses direction. At the open end of the tubes, this reverse flow pulls in pure air from the atmosphere and creates a lean mixture near the cross-over tube. This is a large reason why re-transition was not seen in the test section as is detailed in this section.

The second test series held fill fraction, purge fraction and equivalence ratio for each fuel constant as seen in Table 7. To study the transition of a detonation through the cross-over tube the cross-over width, cross-over geometry and fuels were varied.

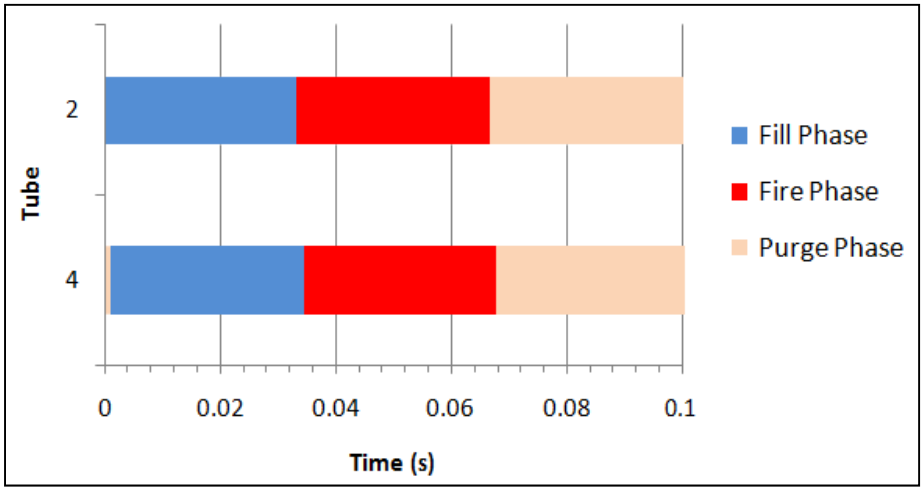


Figure 34. PDE phase offset for tubes 2 and 4 with custom camshaft. Approximately 31.9 ms of overlap for each phase.

Table 7. Experimental constants for second test series

| **Constant** | **Value** |
|---|---|
| Fill fraction | 1.1 |
| Purge fraction | 0.5 |
| Equivalence ratio ($H_2$) | 1.1 |
| Equivalence ratio ($C_2H_4$) | 1.2 |

The first runs (Table 8) in the 2nd test series were run with the rectangular crossover section at varying widths. Runs one through four used hydrogen (φ = 1.1, delay = 2.4 ms) and runs five through eight used ethylene (φ = 1.2, delay = 6.4 ms). The spark delay was adjusted to account for the ignition time of the different fuels and the four degree offset between tubes 2 and 4 in camshaft activation. Wave speeds for hydrogen were very close to the specified CJ speed at position A (Table 8). This proved that detonations up to the cross-over tube were possible with this setup and that the round tube to square tube transition was not an issue. The runs with ethylene never reached CJ speed. Wave speeds decreased through the cross over (position B) and into tube 2 (position D) for both gases. Position C was not of interest for this test series and was not calculated.

Table 8. Average wave speeds through test section using the custom camshaft and rectangular cross-over.

| | | | **Average Wave Speed* (m/s)** (Locations reference Fig. 31) | | |
|---|---|---|---|---|---|
| **Run** | **cross-over width (in)** | **Fuel** | **A** | **B** | **D** |
| 1 | 2 | $H_2$ | 1855 | 905 | 938 |
| 2 | 1.5 | $H_2$ | 1902 | 1102 | 766 |
| 3 | 1 | $H_2$ | 1916 | 1094 | 558 |
| 4 | 0.5 | $H_2$ | 1958 | 994 | 410 |
| 5 | 0.5 | $C_2H_4$ | 1556 | 1028 | 364 |
| 6 | 1 | $C_2H_4$ | 1319 | 804 | 355 |
| 7 | 1.5 | $C_2H_4$ | 1455 | 888 | 727 |
| 8 | 2 | $C_2H_4$ | 1427 | 727 | 622 |
| *($V_{CJ}$ for $H_2$ = 1971 m/s, $C_2H_4$ = 1850 m/s) | | | | | |

A representative sequence of the detonation propagation is shown in schlieren photographs recorded with a rectangular cross-over section and the custom camshaft in Fig. 35. The second frame in Fig. 35 shows a detonation entering the bottom of the test section from left

to right. This is characterized by the planar leading edge of the wave, essentially perpendicular to the walls. The third frame shows that as the detonation expands into the cross over tube it immediately diffracts and begins to transition into a spherical detonation. Since the initial tube diameter is less than ten times the cell width, the transverse wave interactions cannot overcome the expansion and the shock wave and combustion front decouple (Frames 3-5). In frame four a second wave front has developed on the upper right surface of the cross-over tube. This may be a re-initiation of the detonation and would be the expected position of it[8] (Fig. 2). This re-initiation event is not seen in the next frame and has no visible effect on the wave structure coming out of the cross-over tube. The decoupled shock wave and combustion front undergo another expansion into tube 2 and exit the field of view as a high-speed deflagration, based on the calculated wave speeds and images. Wave speeds calculated from these photographs are reported in Table 8. All runs were visually very similar. It was observed that the smaller the cross-over tube, the greater the decoupling of the two fronts coming out of the cross over tube.

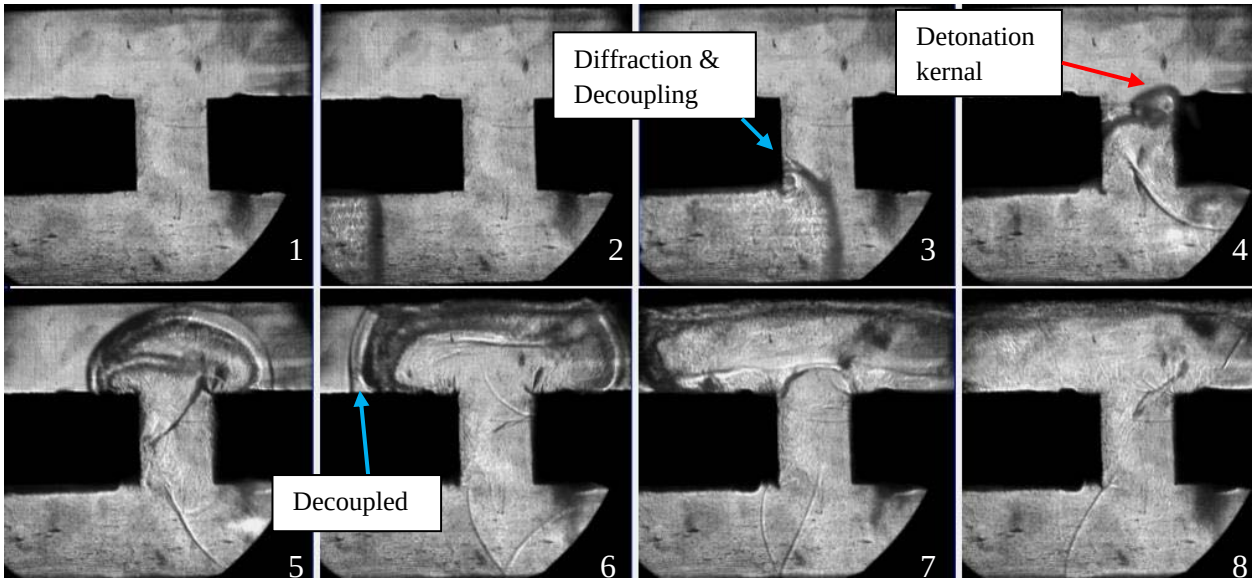


Figure 35. A detonation that diffracts and decouples as it enters the rectangular cross-over section, leaves the frame as a strong deflagration (Run 2, Table 8). Time is from left to right, top to bottom; detonation enters the bottom tube from left to right.

For the next set of runs different geometries were added to the cross-over tube (Fig. 23). The same test constants were kept as in Table 7. Ethylene was used for runs one through four with a delay of 6.4 ms and φ = 1.2. Hydrogen was used for runs five through twelve with φ = 1.1. For runs five through eight a delay of 6.4 ms was used, for runs nine through twelve a delay of 2.4 ms was used. With the added geometry the largest cross-over distance attainable was 1.7". Cross-over width was measured at the midpoint of the geometries.

Table 9 shows wave speeds for the described setup. These wave speeds were again calculated with the schlieren photographs and are reported as an average of the detonations captured in each run.

Table 9. Average wave speeds through the test section using the custom camshaft and varying geometry.

| | | | | | **Average Wave Speed (m/s)** (Locations reference Fig. 31) | | |
|---|---|---|---|---|---|---|---|
| **Run** | **Geometry** | **Fuel** | **Spark Delay (ms)** | **cross-over width (in)** | **A** | **B** | **D** |
| 1 | S | $C_2H_4$ | 6.4 | 1.5 | 1417 | 791 | 550 |
| 2 | S | $C_2H_4$ | 6.4 | 1 | 1417 | 681 | 588 |
| 3 | S | $C_2H_4$ | 6.4 | 1.7 | 1421 | 787 | 744 |
| 4 | S | $C_2H_4$ | 6.4 | 0.5 | 1463 | 888 | 507 |
| 5 | S | $H_2$ | 6.4 | 0.5 | 1601 | 930 | 417 |
| 6 | S | $H_2$ | 6.4 | 1.7 | 1573 | 715 | 757 |
| 7 | S | $H_2$ | 6.4 | 1.5 | 1552 | 808 | 740 |
| 8 | S | $H_2$ | 6.4 | 1 | 1616 | 837 | 600 |
| 9 | U | $H_2$ | 2.4 | 1.7 | 1835 | 677 | 964 |
| 10 | U | $H_2$ | 2.4 | 1.5 | 1835 | 939 | 1116 |
| 11 | U | $H_2$ | 2.4 | 1 | 1827 | 1116 | 706 |
| 12 | U | $H_2$ | 2.4 | 1 | 1872 | 1116 | 913 |
| *($V_{CJ}$ for $H_2$ = 1971 m/s, $C_2H_4$ = 1850 m/s) | | | | | | | |

The ethylene runs (1-4) never achieved CJ speed, while only the 2.4 ms delay runs of hydrogen (9-12) achieved CJ speed. This further shows the significance of small changes in spark delay. In all but one case, the "S" geometry wave speeds continually decrease through the cross-over and into tube 2. The wave speeds in runs nine and ten using the "U" shape geometry increase in tube 2. Though it should be noted that this increase is within the uncertainty for the wave speed calculation.

The runs with the "S" geometry were not at C-J speed entering the cross-over, due to the different spark delay. This reduced wave speed had an effect on the transition of the combustion front and shock wave through the cross-over tube and into tube 2. Geometry "S" did help ease the wave fronts in their expansions, but since it was a subcritical spherical detonation wave it still diffracted and decoupled.

As with the "S" shape geometry, the entrance into the cross-over tube is helped with the "U" shaped geometry, but the cross-over tube is not long enough to allow for the turning and re-initiation as expected. The lip on the upper portion of the "U" does help to trip the detonation and creates a pocket of re-initiation. But this does not transition into a detonation out of the cross-over. The combustion front and shock wave for the "U" shape are nearly coupled in tube 2 (Fig. 36), much closer than with the rectangular or "S" shape geometries (Fig. 37).

In many of the frames in Figs. 36 and 37 dark spots or lines can be seen in the cross-over tube before the detonation has reached the cross-over tube. These are scratches from moving the geometry back and forth in the test section. The scratches block or scatter the light rays, thus making them dark to the camera. The scratches do not hinder the analysis of the detonation as it travels through the cross-over tube.

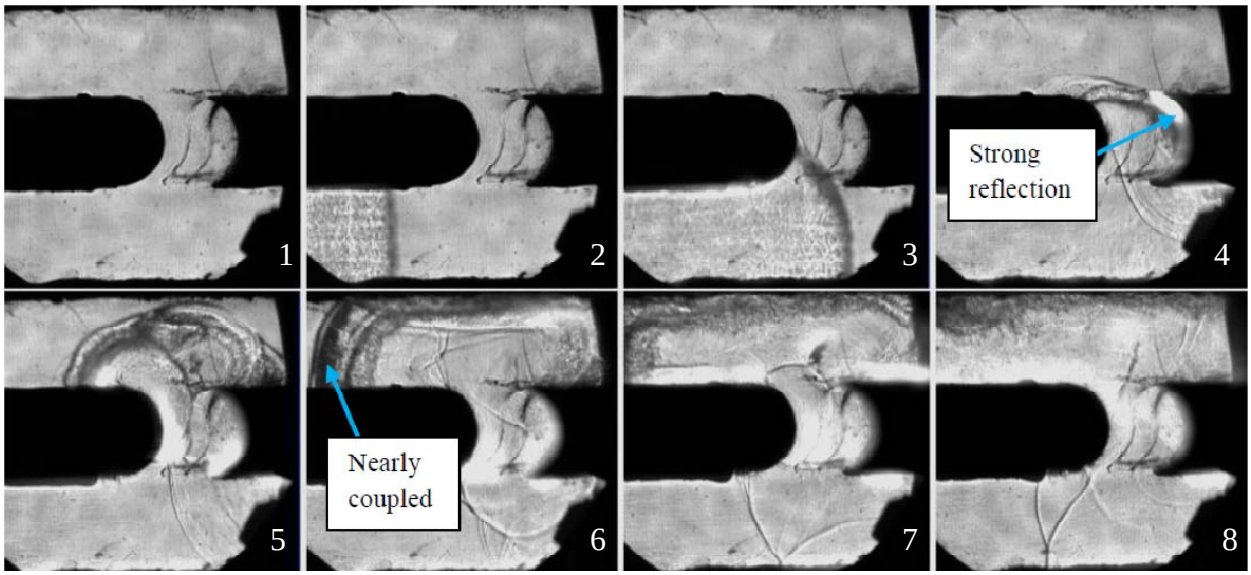


Figure 36. Detonation entering the "U" shaped geometry, decoupling is lessened into the cross-over. (Run 10, Table 9) Time is from left to right, top to bottom; detonation enters the bottom tube from left to right.

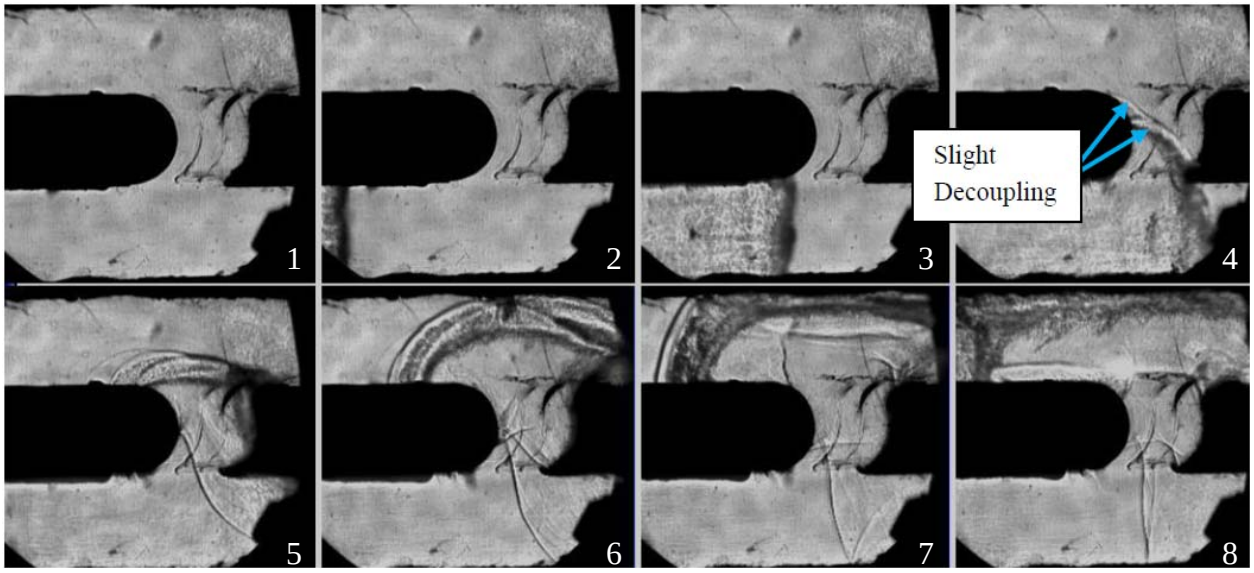


Figure 37. Weak detonation entering the "S" shaped geometry, decoupling into and out of the cross-over. (Run 7, Table 9) Time is from left to right, top to bottom; detonation enters the bottom tube from left to right.

The modified "U" geometry was installed in the cross-over tube next. Frame 2 of Figure 38 shows the same event that was seen on the upper portion of the u-shape in Fig. 36.

The re-initiation event on the inside of the cross-over in frame three is a reflection of the same event in frame two. This means that there is no strong reaction happening on the inside of the cross-over tube, even with the many obstacles. Though there are energetic events occurring in the cross-over tube, the gases expand again into tube 2 and these localized pockets of re-initiation are not seen again.

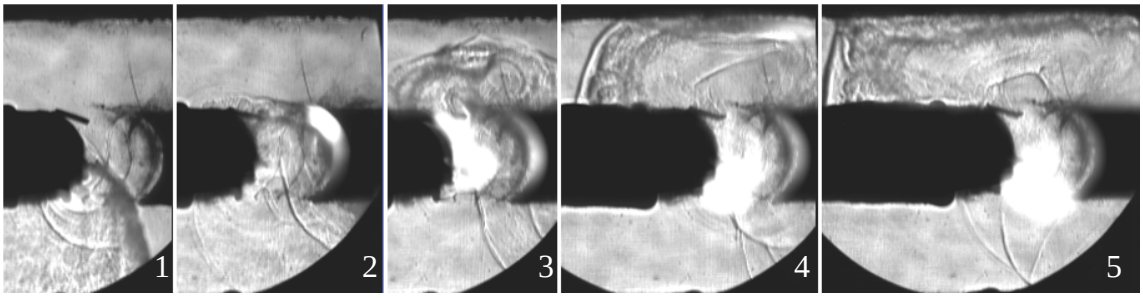


Figure 38. Modified "U" geometry does not cause a detonation in tube 2. Time is from left to right; detonation enters the bottom tube from left to right.

In all the of runs for the 2nd test series a detonation was not re-initiated in tube 2 before the detonation front exited the field of view of the camera. It is clear that the detonation did re-initiate as the ion probes upstream in tube 2 did measure CJ speeds for 100% (6/6) of the hydrogen runs with the "U" shape and 75% (3/4) of the hydrogen runs with the "S" shaped geometry. For the rectangular geometry 75% (3/4) of the hydrogen runs re-transitioned. None of the runs (0/4) with hydrogen transitioned with the modified "U" shape. Average wave speeds from the ion probes are shown in Fig. 39. Appendix C contains the full test matrix for the 2nd test series. Appendix B contains a discussion of why only the CJ wave speeds that were calculated by the ion probes upstream in tube 2 are reported here.

The run that did not transition for the rectangular portion was the 0.5" cross-over width case. This is a clear message that there are cross-over size limits in transferring a detonation to another tube (Fig. 39). Though the "S" shape geometry did not attain C-J wave speeds into the

cross-over, it did re-transition. This shows that there is less dependence on the initial detonation coming into the cross-over tube. This may be due to the fact that the detonation decouples in all cases through the cross-over tube and therefore has to re-transition in all cases. The intent will now be to re-transition the detonation as quickly as possible out of the cross-over tube since it slows and decouples in all cases.

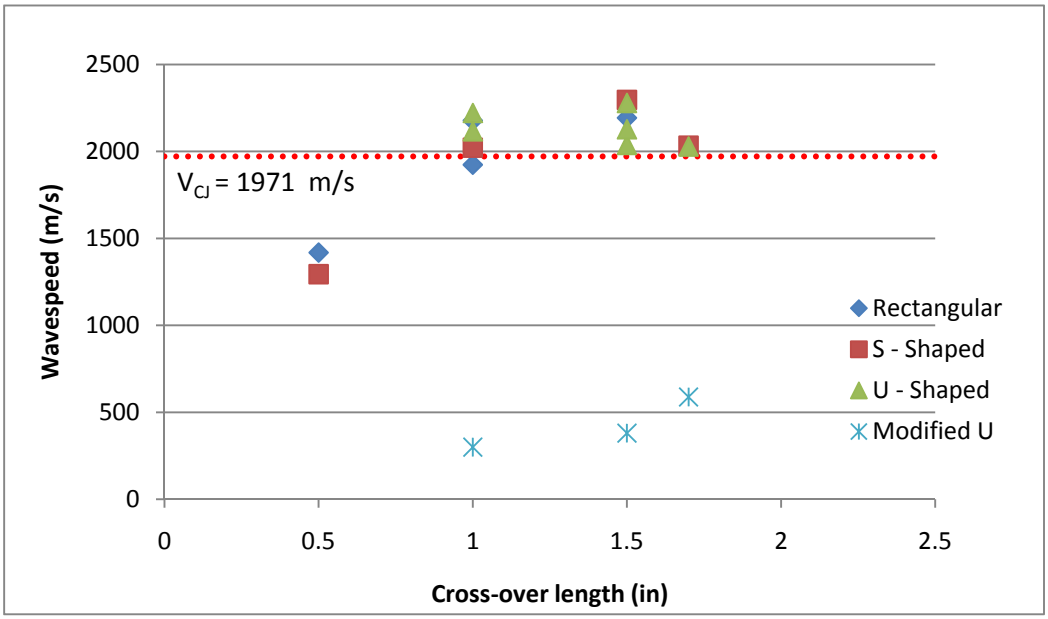


Figure 39. Average wave speeds measured 30-40" from PDE head by ion probes for each run in test series two.

The 2nd test series showed there are limits to the size of the cross-over and this appears to be on the order of at least one cell size. It is possible to delay the decoupling of the shock wave and combustion front, but in this setup it does not appear that there is a way to stop it. It also appears that any energy taken from the waves in the cross-over tube is harmful as none of the runs with the modified "U" geometry re-transitioned upstream in tube 2. With the PDE head used for this research, an air-spring will always be present. This must be mitigated with proper placement of the cross-over tube or a device that does not allow pure air to be pulled into the detonation tube.

### 3. Test Series 3

The 3rd and final test series looked at tripping the waves back to a detonation at the exit of the cross-over tube and into tube 2. The goal was to see if re-initiation can happen quicker than in test series 2, which was re-initiated outside of the test section. It was noted that in all previous runs there was decoupling entering and exiting the cross-over tube. With this in mind the 3rd test series will try to delay the expansion and decoupling into the cross-over tube, but not stop it. The focus will be on re-initiating the detonation at the second expansion, into tube 2.

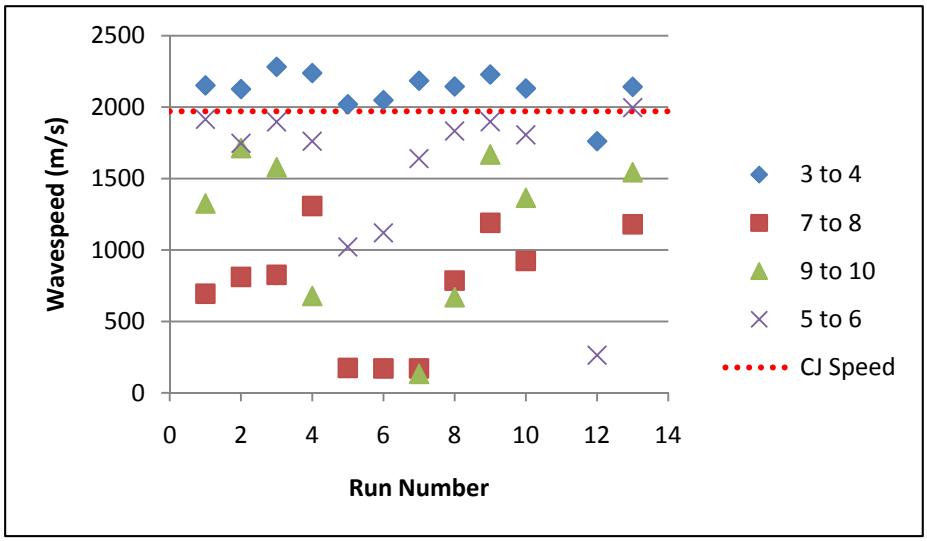


Figure 40. Average wave speeds calculated from the ion probes in the test section for the baseline run of the 3rd test series

The same "U" geometry cross-over setup used in test series 2 was used in test series 3 to provide a baseline for the single tube PDE setup before obstacles were installed in the test section. Hydrogen was used as fuel with a fill fraction of 1.3 to ensure the upper tube (tube 2) in the test section was adequately filled with detonable mixture. With the single tube setup there is no question as to if the cross-over tube is filled, the filling can be viewed via the schlieren photography. Only a slight restriction on tube 4 was needed to fill tube 2 as detonations occurred in tube 2 with the 0.5" nozzle and the 1.0" nozzle, with seemingly no

difference in the performance of either.

Figure 40 is a graph of wave speeds calculated from the ion probes at locations denoted in Fig. 30. As expected, the detonation decays through the cross-over tube, but with this setup quickly regains speed in the test section. As it leaves the test section (probes 9 to 10) it is near CJ speed. The parameters for each run are shown in Table 10. At smaller cross-over widths wave speeds drop significantly through the cross-over and out of the test section.

Table 10. Parameters for baseline tests of 3rd test series

| Run # | Delay (ms) | x-over width (in) | Equivalence Ratio | Fill Fraction | Nozzle |
|---|---|---|---|---|---|
| 1 | 2.4 | 1.7 | 1.1 | 1.2 | .5" |
| 2 | 2.4 | 1.7 | 1.1 | 1.3 | .5" |
| 3 | 2.4 | 1.7 | 1.1 | 1.3 | .5" |
| 4 | 2.4 | 1.2 | 1.1 | 1.3 | .5" |
| 5 | 2.4 | 0.7 | 1.1 | 1.3 | .5" |
| 6 | 2.4 | 0.7 | 1.1 | 1.3 | .5" |
| 7 | 2.4 | 0.7 | 1.1 | 1.3 | .5" |
| 8 | 2.4 | 1.2 | 1.1 | 1.3 | .5" |
| 9 | 2.4 | 1.7 | 1.1 | 1.3 | .5" |
| 10 | 2.4 | 1.7 | 1.1 | 1.3 | .5" |
| 11 | 2.4 | 1.7 | 1.1 | 1.3 | 1" |
| 12 | 2.4 | 1.7 | 1.1 | 1.3 | None |
| 13 | 2.4 | 1.7 | 1.1 | 1.1 | 1" |

Detonations were seen in the upstream window of the test section with this baseline setup for a 1.7” cross-over width. The images seen in this setup are drastically different than those of the same test section configuration in test series 2, they are much more energetic (a full test matrix is found in Appendix C). Figure 41 is a composite figure of a run where the camera was pointed at the cross-over area of the test section and where the camera was pointed at an upstream position. Each run had the same parameters, but it must be made clear that these were two completely different runs separated by up to an hour in time.

A strong reflection from the ceiling of the test section tube is clearly seen in frame 5, this then propagates down to the bottom of the tube in frame 6 as the front of the waves leave the field of view. Due to combination of two different runs, frames 6 and 7 would mostly likely occur at the same moment in time. The planar detonation structure has returned in frame 8 and the high velocity detonation quickly leaves the field of view by the last frame. All the runs that detonated in the test section in the baseline setup are characterized by a strong reflection on the top wall of the test section followed by a very strong reflection on the lower surface of tube 2.

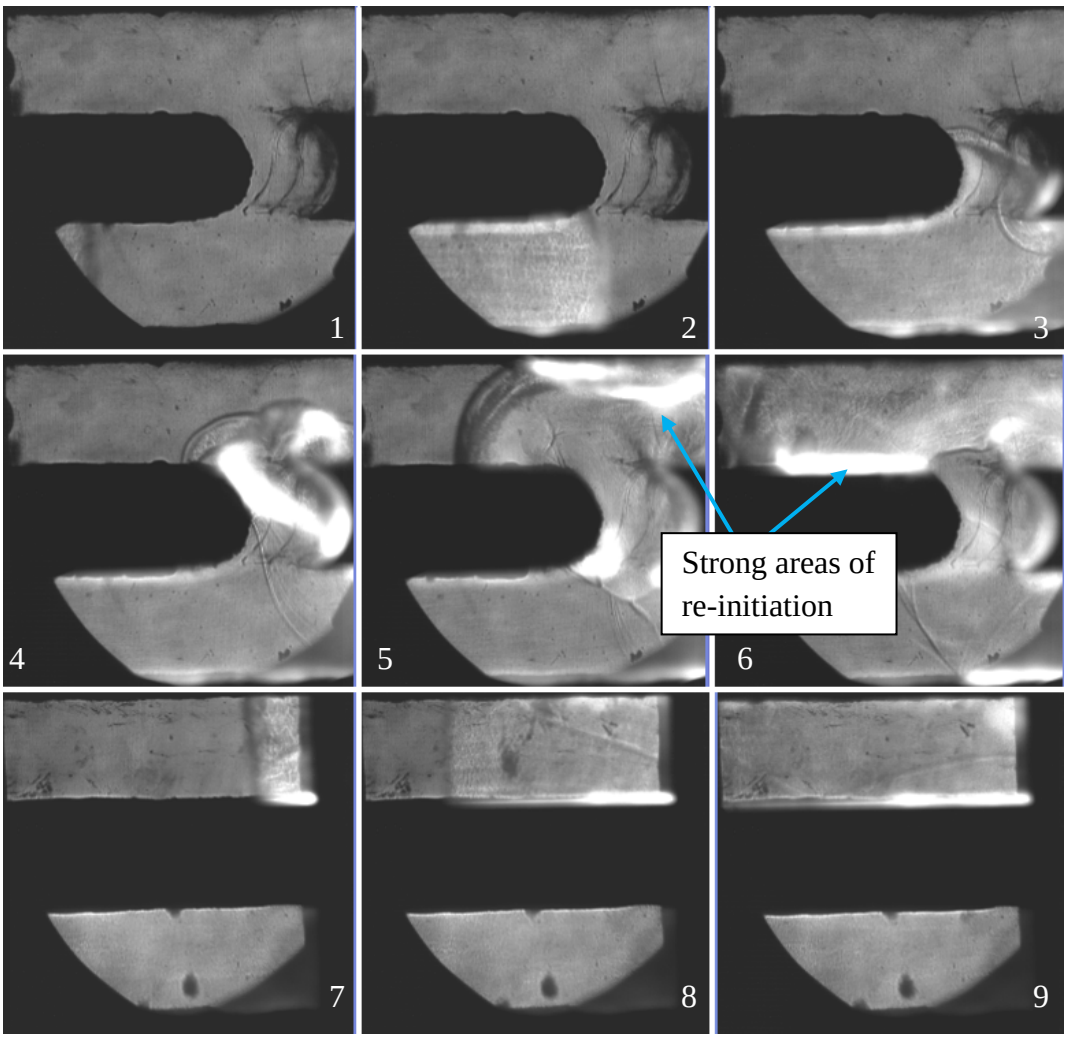


Figure 41. Composite pictures of two different runs at both the cross-over viewing location (1-6) and the upstream viewing location (7-9). Each run had the same parameters. A detonation has re-initiated in frame 8. Detonation enters the bottom tube from left to right.

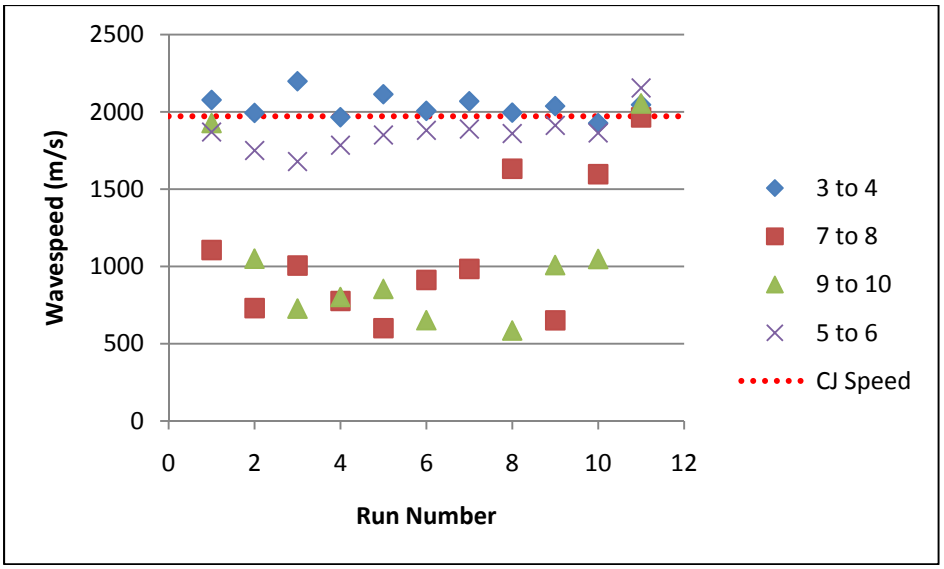

Figure 42. Average wave speeds from ion probe data for various test section configurations

Table 11. Parameters for runs with obstacles and varying cross-over configurations

| Run # | Delay (ms) | Geometry | x-over width (in) | Equivalence Ratio | Fill Fraction | Nozzle |
|---|---|---|---|---|---|---|
| 1 | 2.4 | U w/obs | 1.7 | 1.1 | 1.3 | 1" |
| 2 | 2.4 | U w/obs | 1.7 | 1.1 | 1.3 | .5" |
| 3 | 2.4 | U w/obs | 1.2 | 1.1 | 1.3 | .5" |
| 4 | 2.4 | U w/obs | 1.2 | 1.1 | 1.3 | .5" |
| 5 | 2.4 | U w/obs | 1.7 | 1.1 | 1.3 | .5" |
| 6 | 2.4 | U w/obs | 1.7 | 1.1 | 1.3 | .5" |
| 7 | 2.4 | U w/obs* | 1.7 | 1.1 | 1.3 | .5" |
| 8 | 2.4 | U | 1.7 | 1.1 | 1.3 | .5" |
| 9 | 2.4 | U | 1.7 | 1.1 | 1.3 | .5" |
| 10 | 2.4 | U | 1.7 | 1.1 | 1.3 | .5" |
| 11 | 2.4 | D** | 1.7 | 1.1 | 1.3 | .5" |

*cross-over obstacle taken off
**U geometry removed from right side, semi-circle on left side remained

When the static mixers, or obstacles, were added to the test section the re-initiation process was hindered. This is seen in Fig. 42 as wave speeds in tube 2 for the runs with obstacles never reach above 1200 m/s. Run parameters are displayed in Table 11. The obstacles were large enough that they trapped the reflection on the bottom wall and it can be seen

bouncing back and forth between the obstacles vertically and horizontally in the schlieren images presented in this section and in Appendix A. The issue is that, while the obstacles are producing reflections as desired, they not allowing the detonation to continue in the axial direction after the detonation has been re-initiated. Figure 43 is a good example of how the energy from the detonation has been trapped in the obstacles. It does not have a chance to leave and can be seen bouncing from top to bottom while trapped in the obstacles in frames 6-12. The obstacles were removed due to their ineffectiveness in re-initiating a detonation in the axial direction.

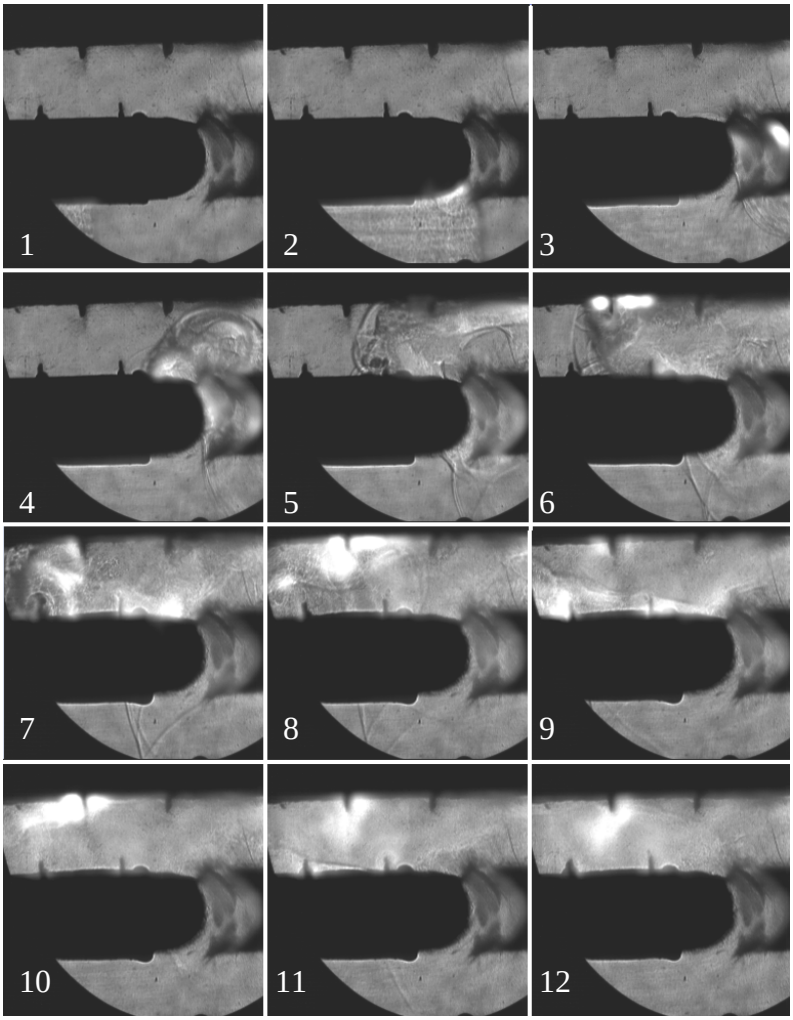


Figure 43. The detonation has a strong reflection off of the top wall but is then trapped by the obstacles. A reaction can be seen reflecting top to bottom in frames 6-12. Time is from left to right, top to bottom; detonation enters the bottom tube from left to right.

Detonations only occurred in the test section for the largest cross-over width, 1.7". The smaller widths seem to restrict the waves enough that a strong reflection from the top wall is not achievable. Pockets of re-initiation similar to the 1.7" case are seen off of the U-shape in the cross-over tube and in the middle of tube 2, but they do not initiate the required reaction on the top of tube 2.

The runs in which the schlieren light source was turned off are quite telling. The reflections are obvious and two notable reflections take place, one in the cross-over tube from the outside to the inside and one from the top of tube 2 above the cross-over to the bottom of tube 2 just upstream of the cross-over. The latter, referred to above seems to be the mechanism of transition for the waves in the cross-over tube.

For the last run, the U-shaped obstacle was taken off, but the inside semi-circle was left on. This provided the most promising run and is shown in Fig. 44. The right side of the cross-over tube is aligned with the extreme right edge of the photographs. While it may not be clear to the observer, there is no missing information in these pictures, the entire cross-over is visible. Additionally, scratches and melting of the polycarbonate has made the actual cross-over difficult to see, but for these pictures it is of no consequence. The detonation reflects off of the outside of the cross-over tube in frame two, then has a strong and uniform reflection off of the top of the test section in frame 3 and has re-transitioned to a detonation and leaves the viewing area. There is no additional reflection seen along the bottom as with the "U" shape geometry, only one reflection is needed.

The U-shape, while creating a reflection could have actually been hindering the process of re-transition. The semi-circle inside provides for an easier transition around the 180 degree turn, and no slow down or energy is taken from the waves on the outside of the obstacle. This

allows for a stronger reflection on the ceiling of tube 2, higher speeds and a much quicker transition to detonation.

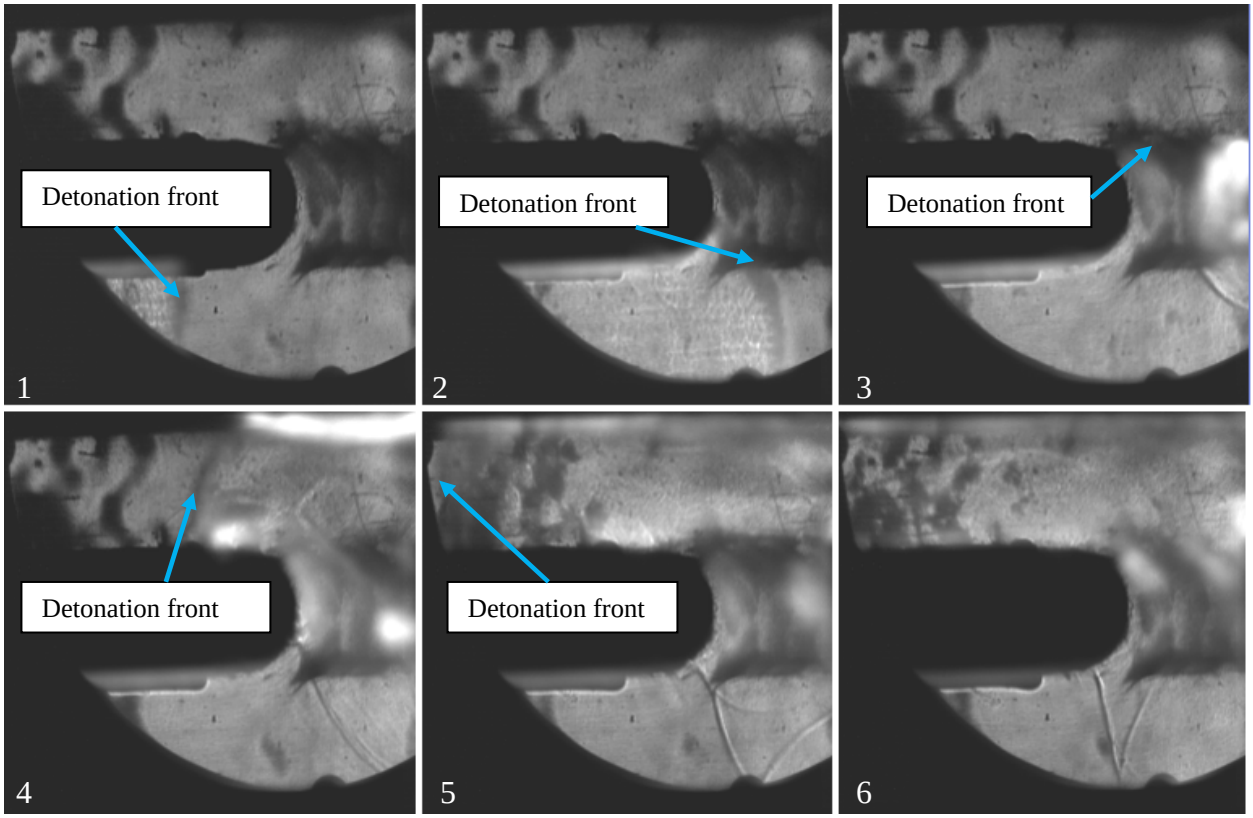


Figure 44. Run with no geometry on outside of cross-over tube. Only run to transition in the field of view of the cross-over section. Time is from left to right, top to bottom; detonation enters the bottom tube from left to right.

The ion probes located after the cross-over section in tube 4 (Locations 5 & 6 in Fig. 30) do record CJ speed, or very near it as seen in Fig. 45. This is important as it definitively shows that the cross-over tube does not end the original detonation. Generally wave speeds drop by approximately 100-200 m/s just after the cross-over. This is most likely due to the diffraction that has taken place. As the detonation passes the cross-over tube opening there is noticeable curvature in the front. This will take a short distance to become planar once again and regain the speed it momentarily lost due to the cross-over opening. If the ion probes were further downstream, they would likely read a higher velocity.

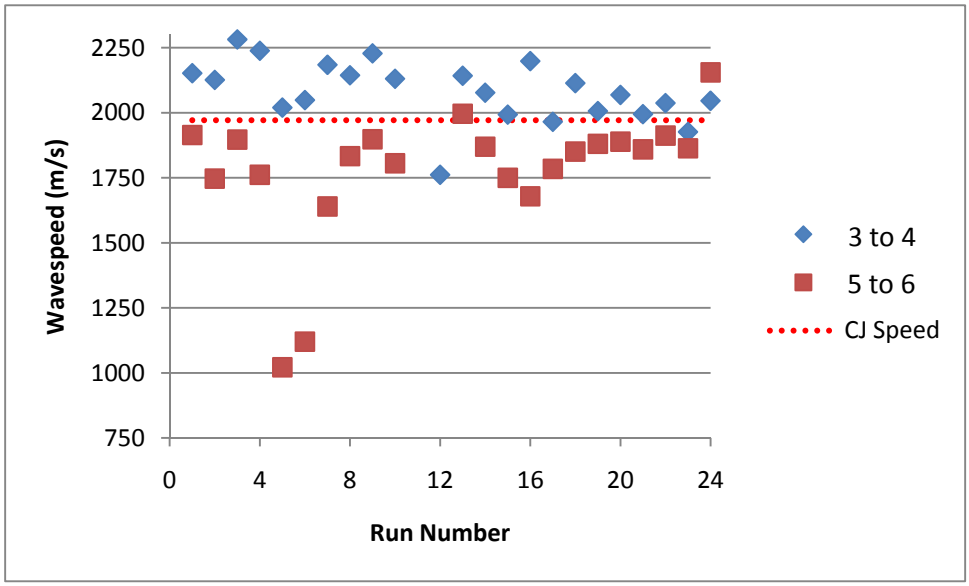


Figure 45. Wave speeds into and out of tube 4 for test series 3

As can be seen from the schlieren imagery the windows in the cross over section started to become less transparent as the runs went along. This is because the polycarbonate started to melt on the outside of the cross-over tube. This is another indication of the strong events taking place in the cross-over tube. Though there were only five detonation events and adequate time to cool between runs, melting occurred. Figure 46 shows the melting. Each spot of melt corresponds to a different location of the U-shape. There were no issues on the inside of the cross-over tube indicating that the stronger event happened at the outside of the cross-over tube.

The 3rd test series proved that re-initiation immediately out of the cross-over tube is possible by a strong reflection of the top wall of tube 2. The outside portion of the cross-over tube is where the strongest reactions occur, indicating it is this portion of the wave that is responsible for the strong reaction in tube 2. Since it is not the reactions inside the cross-over tube that are re-initiating the detonation, cross-over tubes should be made with as few obstacles

and restrictions as possible. Finally, cross-over width is important with only the 1.7” case providing a detonation in the test section.

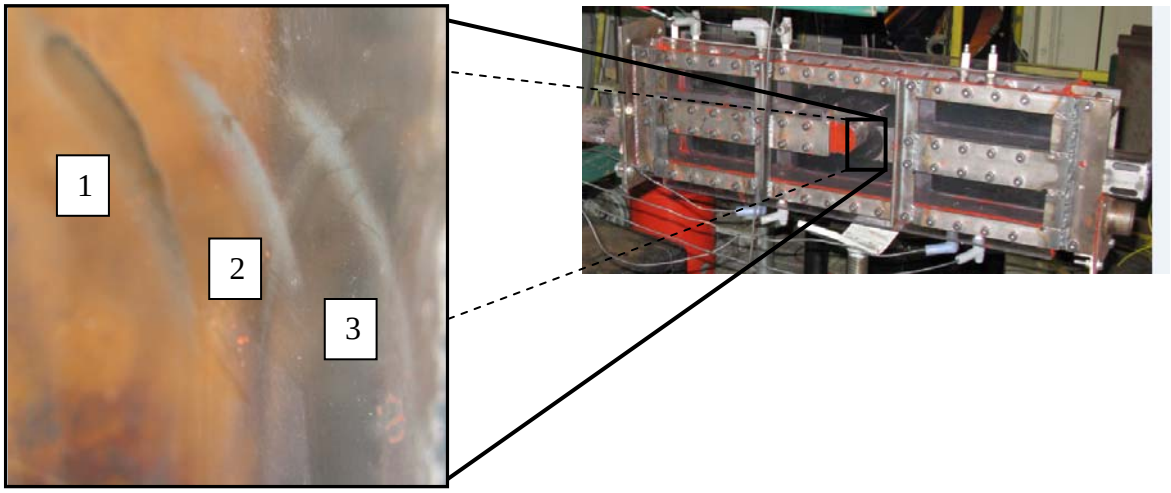


Figure 46. Melting of polycarbonate in third test series. Three spots correspond to the three cross-over locations used.

Table 12. is presented as a summary of all configurations and runs reported in this section. The column labeled ‘Near PDE head in tube 2’ refers to wave speed measurements recorded by the ion probes that were placed 30” and 40” from the PDE. The column ‘In test section’ refers to measurements recorded by ion probes installed in the test section or schlieren images from the test section. Average wave speeds calculated that were within 15% of CJ speed were considered to have re-transitioned.

Table 12. Results Summary

| Test Series | # of tubes used for fill/purge | Camshaft | Fuel | Cross-over width (in) | Geometry | Obstacles in Tube 2 | Nozzle on Tube 4 | Re-initiation | |
|---|---|---|---|---|---|---|---|---|---|
| | | | | | | | | Near PDE head in Tube 2 | In test section |
| 1 | 2 | Stock | Hydrogen | 1.0 - 2.0 | Rectangular | None | None | **Yes** | No |
| | | | Ethylene | 1.35 - 2.0 | Rectangular | | | No | No |
| 2 | 2 | Custom | Hydrogen | 0.5 | Rectangular | None | None | No | No |
| | | | | 1.0 - 2.0 | Rectangular | | | **Yes** | No |
| | | | | 0.5 - 1.7 | S | | | **Yes** | No |
| | | | | 1.0 - 1.7 | U | | | **Yes** | No |
| | | | | 1.0 - 1.7 | mod-U | | | No | No |
| | | | Ethylene | 0.5 - 2.0 | Rectangular | | | No | No |
| | | | | 0.5 - 1.7 | S | | | No | No |
| 3 | 1 | Stock | Hydrogen | 0.7 - 1.2 | U | None | 1" | N/A | No |
| | | | | 1.7 | U | None | | | **Yes** |
| | | | | | U | Yes | | | No |
| | | | | | D | None | | | **Yes** |

# V. Conclusions

The detonation propagation through a cross-over tube of different sizes and geometries was visualized with the use of schlieren photography. The visualization helped determine important characteristics of tube-to-tube initiation.

First, since all tubes are connected, they will affect one another. This interaction must be taken into account to ensure all tubes are filled with the proper mixture when ignition takes place. Spark timing is an important parameter in the engine setup to ensure all tubes are at the desired point in their respective cycles when ignition happens. It is also important to know that the cross-over tube is being completely filled with mixture at the desired equivalence ratio.

For the test configuration used in this research, the detonation wave, traveling at C-J speed, is required to turn 180 degrees in a short distance. As the wave enters the cross-over tube there is immediate diffraction and it begins to transition into the cross-over volume as a sub-critical spherical detonation, as the tube height is not greater than 10λ. It was shown that strong reflections and pockets of detonation re-initiation could be achieved in the cross-over tube. However, these did not make it out of the cross-over tube as another expansion is required at the exit of the cross-over tube. Therefore, it has been shown that there is little to be gained at the entrance of the cross-over tube. It was shown that a smooth transition into the cross-over led to a delay in the decoupling of the shock wave.

When a re-initiation of a detonation was observed in the test section, the mechanism of re-initiation was a strong reflection off of the top wall in tube 2. The most promising of the re-initiation cases was with no obstacle on the outside of the cross-over tube. This leads to the result that as little energy as possible should be taken away from the fronts passing through the cross-over tube. The “U”-shape geometry took away energy in the cross-over tube by the

reflection on its upper surface. The points of interest will be on the inside of the cross-over tube, to reduce the expansion of the detonation wave coming into the cross-over tube. Also, the outside of the cross-over tube will be important to not take energy away from the waves. The next reflection that the shock and combustion wave experience is critical, a strong reflection on the outside tube wall or on an obstacle parallel to the main detonation tube that allows for the reflected waves to travel uninhibited upstream in the detonation tube will provide the best conditions for successful initiation.

There are limits to the cross-over width, with narrower cross-over sections not re-transitioning the detonation. This is because of the energy taken out of the waves through the cross-over tube, there is not enough to then reach the top of tube 2 and create re-initiation. Obstacles may help transition the waves if placed in optimal positions. It is clear from this research that the fronts should not be slowed down by obstacles as they tend to trap the strong reactions as the fronts travel down the detonation tube.

Obstacles in the initiated tube do show promise. For placement of obstacles the author would recommend one on the inside very near to the exit of the cross-over and one on the top with a gap and placed an inch or more downstream. This allows for a strong reflection on top, but also a place for the gases to exit. It also adds a place for the detonation to 'push-off' from on the bottom and does not restrict its movement in the upstream direction. It appears that this obstacle does not need to be very large and could be less than the 3/8" that was tested in this research.

In terms of losses, it was shown that a detonation can be initiated directly after it comes out of the cross-over tube, this ensures the most amount of fuel being used for detonation. It was

also shown that smaller cross-over tubes than the diameter of the main detonation tubes can be successful, thus reducing the required fill.

**1. Future work**

Based on the conclusions from this research there are numerous recommendations for future work. First, the "D" shape geometry should be further studied with the test series 3 setup to determine if smaller cross-over widths will allow for the re-transition of a detonation in the test section. Also, ethylene should be used to determine if it would also work with the test series 3 setup and the D shape.

With the visualization of square tubes reported here, round tubes can be looked at and improved upon. It appears that the round tubes had better success than the square tubes[5], so with knowledge of what is happening in the cross-over tube, heavier fuels may be able to be successfully initiated with the benefits from round tubes.

A study to determine optimum detonation tube length and cross-over tube location is necessary to mitigate detonation tube interaction and air-spring effects. Both of these issues affect the equivalence ratio of the fill mixture near the cross-over tube. Small changes in equivalence ratio can cause a detonation to fail.

Since it has been shown that a detonation can re-initiate by reflections, studies should be done to determine the best configuration of the initiated tube near the cross-over tube for optimal transition to include smaller cross-over tubes. This may occur for smaller cross-over tube widths with an obstacle placed in the middle of the initiated tube.

To eliminate equivalence ratio issues, studies should be done to determine the contents of the gases in the cross-over tube. If this turns out to be an issue, cross-over tubes of minimal length may also be looked at to eliminate the chance for these equivalence ratio issues.

For greater fidelity in research parameters a more consistent and accurate method of calculating wave speeds is needed. For combustion speeds that are less than 60% of CJ speed are an issue as the voltage drops are jagged or sloped, leading to inconsistencies in determining the exact time of combustion wave arrival.

The runs without the schlieren light source turned on were very telling to the mechanisms that make the detonations re-transition. Quartz windows should be obtained for the cross-section so C-H filtering can occur and exact ion wavelengths can be measured. Additionally, two cameras or a dual set of mirrors should be used to capture the entire detonation event, from entrance into the test section, through the cross-over tube and out of the test section.

## References


1. Oates, Gordon C. *Aerothermodynamics of Gas Turbine and Rocket Propulsion*. Reston, VA: American Institute of Aeronautics and Astronautics, 1997. Print.

2. Turns, Stephen R. *An Introduction to Combustion: Concepts and Applications*. Boston: WCB/McGraw-Hill, 2000. Print.

3. Hopper, D. R., King, P. I., Schauer, F. R., Katta, V. R., and Hoke, J. L., 2007. "Detonation Propagation across an Asymmetric Step Expansion", AIAA 2007-5078, 43rd AIAA/ASME/SAE/ASEE Joint Propulsion Conference & Exhibit, Cincinnati, OH, 9-12 July 2007.

4. Gilbert, Jonathan M. *Direct Initiation of Multiple Tubes by Detonation Branching in a Pulsed Detonation Engine Using Hydrocarbon Fuels*. MS thesis, AFIT/GAE/ENY/09-M09. Graduate School of Engineering and Management, Air Force Institute of Technology (AU), Wright-Patterson AFB OH, March 2009.

5. Hopper, D. *Direct Initiation of Multiple Tubes By Detonation Branching In a Pulsed Detonation Engine*. Doctoral Dissertation. AFIT/DS/ENY/08-05. Graduate School of Engineering and Management, Air Force Institute of Technology (AU), Wright-Patterson AFB OH, August 2008.

6. Rolling, August J. *Alternative Pulse Detonation Engine Ignition System Investigation through Detonation Splitting*. MS thesis, AFIT/GAE/ENY/02-10. Graduate School of Engineering and Management, Air Force Institute of Technology (AU), Wright-Patterson AFB OH, March 2002 (ADA40512).

7. Thomas, G.O., Williams, R.L. Detonation Interaction with Wedges and Bends. Shock Waves, Vol. 11, No. 6, May 2002, pp. 481-492.

8. Igra, O.,Wang L., Falcovitz, J., and Heilig, W. Shock Wave Propagation in a Branched Duct. Shock Waves, Vol. 8, No. 6, December 1998, pp. 375-381.

9. Feivisohn, Robert T. *Numerical Investigation of Pre-detonator Geometries for PDE Applications*. MS thesis, AFIT/GAE/ENY/10-M09. Graduate School of Engineering and Management, Air Force Institute of Technology (AU), Wright-Patterson AFB OH, March 2010.

10. Sorin, R., Zitoun, R., Khasainov, B., Desbordes, D. Detonation Diffraction Through Different Geometries. Shock Waves, Vol. 19, No. 1, April 2009, pp. 11-23.

11. Gelfand, B.E., Khomik, S.V., Bartenev, A.M.,Medvedev, S.P., Gronig, H., Olivier, H. Detonation and Deflagration Initiation at the Focusing of Shock Waves in Combustible Gaseous Mixture. Shock Waves, Vol. 10, No. 3, July 2000, pp. 197-204.

12. Hopper, D., King, P., Hoke, J., Paxson, D., and Schauer, F. Detonation Initiation and Propagation in a Branched Detonation Pulsed Detonation Engine. JANNAF Journal of Propulsion and Energetics, Vol. 3, No. 1, May 2010, pp. 55-69.

13. Soloukhin, Rem Ivanovich. *Shock Waves and Detonations in Gases,*. Baltimore: Mono Book, 1966. Print.

14. Glassman, Irvin, *Combustion, 3rd Edition*, Academic Press, San Diego, CA, 1996. Print.

15. Guirao, C.M., Knystautas, R., Lee, J., Benedick, W., and Berman, M. Hydrogen-Air Detonations, *19th Symposium (Int.) on Combustion*, pp. 583-590, 1982.

16. Knystautas, R., Guirao, C., Lee, J.H., and Sulmistras, A. Measurements of Cell Size in Hydrocarbon-Air Mixtures and Predictions of Critical Tube Diameter, Critical Initiation Energy, and Detonability Limits, *Progress in Astronautics and Aeronautics*, vol. 94, pp.23-37, 1984.

17. Tucker, K.C., ―A Flash Vaporization System for Detonation of Hydrocarbon Fuels in a Pulse Detonation Engine, PhD Dissertation, Air Force Institute of Technology, WPAFB OH, 2005.

18. "Gas Explosion Handbook." *GexCon AS*. Web. Winter 2011. <http://www.gexcon.com/handbook/GEXHBchap6.htm#sect6.2>.

19. Schultz, E., Detonation Diffraction Through an Abrupt Area Expansion, PhD Dissertation, California Inst. of Tech., Pasadena, CA, 2000.

20. Tavoularis, Stavros. Measurement in fluid mechanics. Cambridge: Cambridge UP, 2005.

21. Stevens, C.A., Gamezo, V.N., King, P.I., Schauer, F.R., Hoke, J.L. 2011. “Interactions of Detonations with Ramps”. AIAA2011-0324, 49th AIAA Aerospace Sciences Meeting, Orlando, FL, 4-7 Jan 2011.

## Appendix A. Schlieren images from the 3rd test series

Page

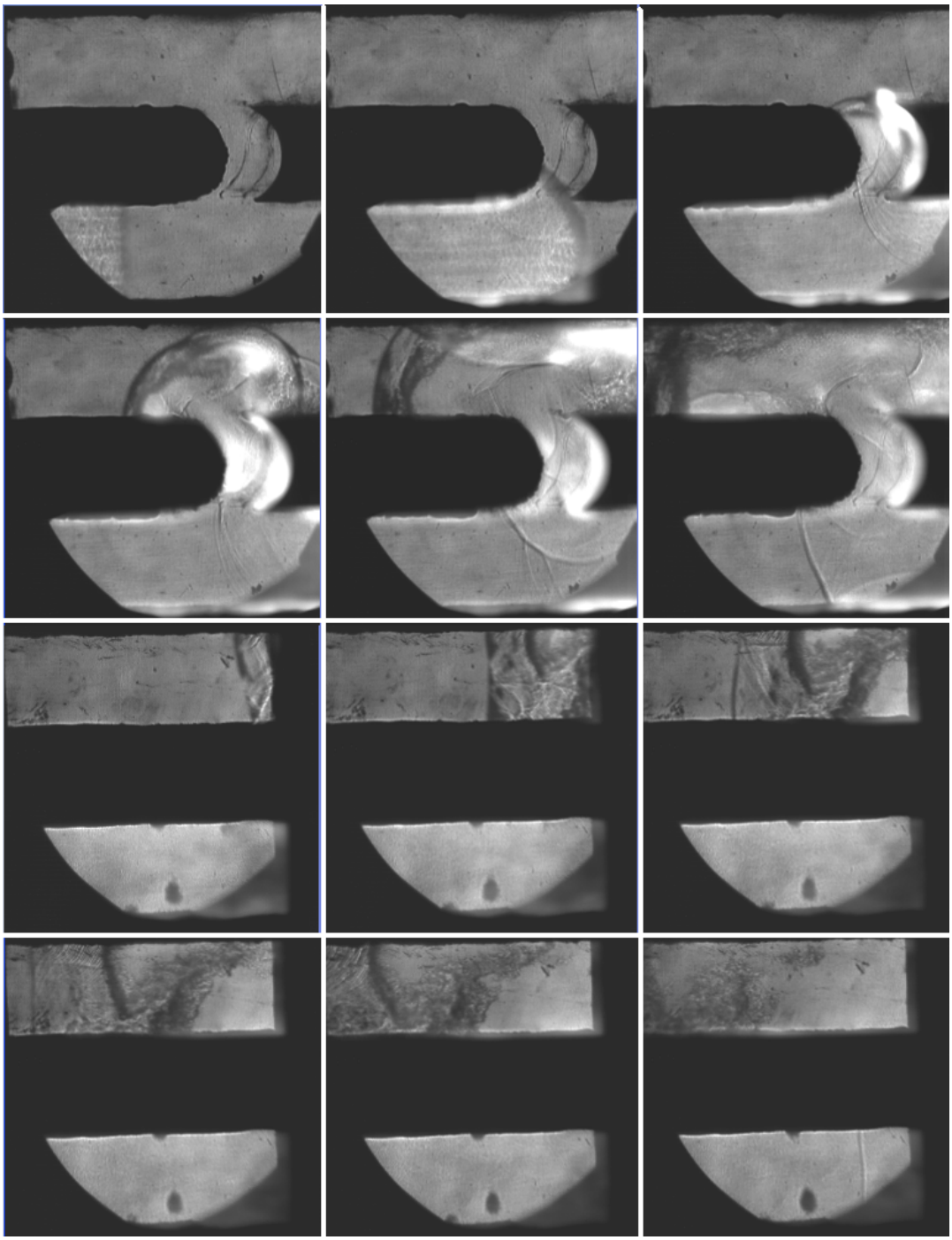

Figure A-1. Image of detonation that does not re-initiate. Cross-over is 1.2” in width. Figure is a composition of two separate runs. Time is from left to right, top to bottom; detonation enters the bottom tube from left to right.

Figure A-1 is a composite of images from runs 4 and 8 on 10 February (see Appendix C).

These runs did not re-transition to a detonation. The frames look similar to the successful

detonation in Fig. 41 but the differences start in frame 5 where there seems to be a strong reflection downstream of the cross-over tube on the top of tube 2, but not upstream of the cross-over tube. There is then no reflection on the bottom and as can clearly be seen in frames 7-12 the shock wave is out ahead of the combustion front and the shock wave decays as it traverses the short eight inches of the field of view.

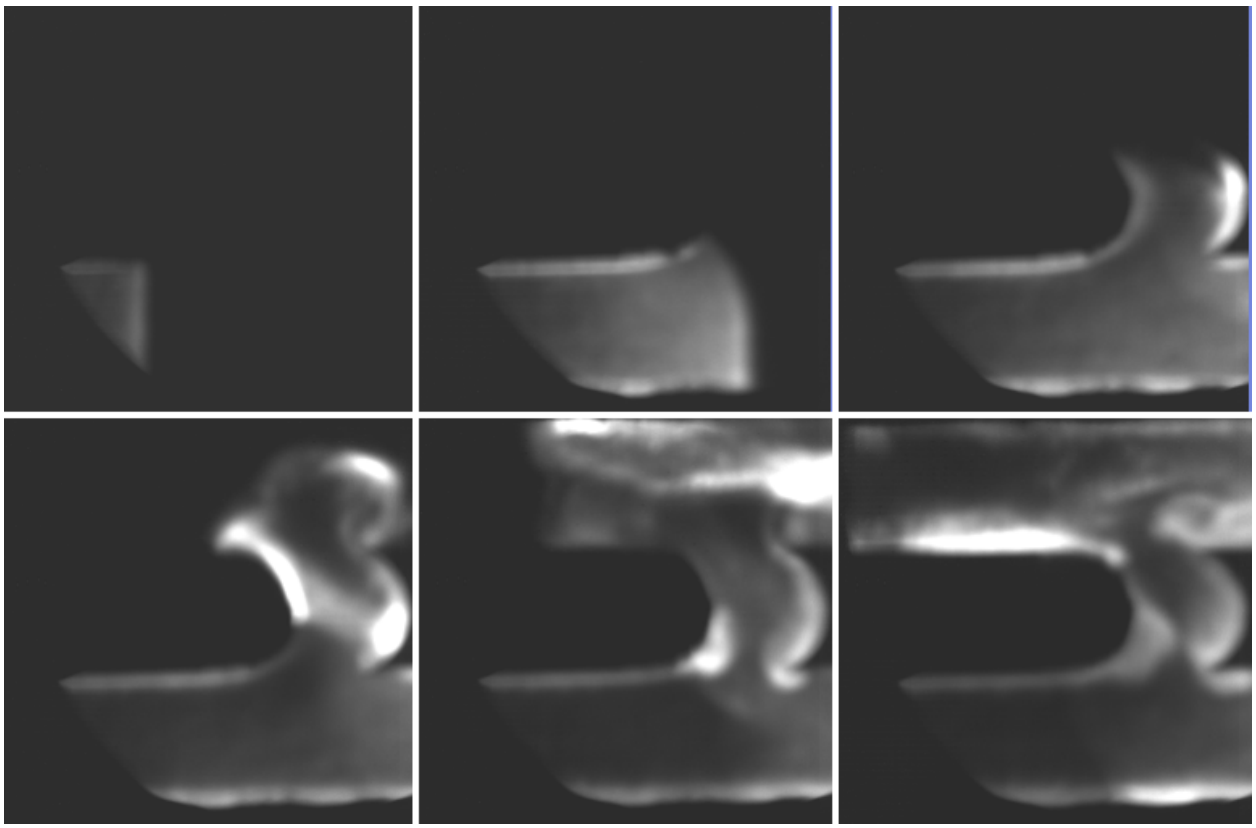

Figure A-2. Successful re-initiation with schlieren light source turned off. Cross-over is 1.2" in width. Time is from left to right, top to bottom; detonation enters the bottom tube from left to right.

Figure A-2 is run with the same conditions as Fig. A-1 and does successfully transition in the test section to a detonation. In frame 4 note that the bright spot on the inside of the cross-over is actually a reflection of the strong reaction on the "U"-shaped geometry on the outside of the cross-over. A strong reflection is seen on the upper wall of tube 2 which leads to a strong reflection on the bottom of the tube and re-transition.

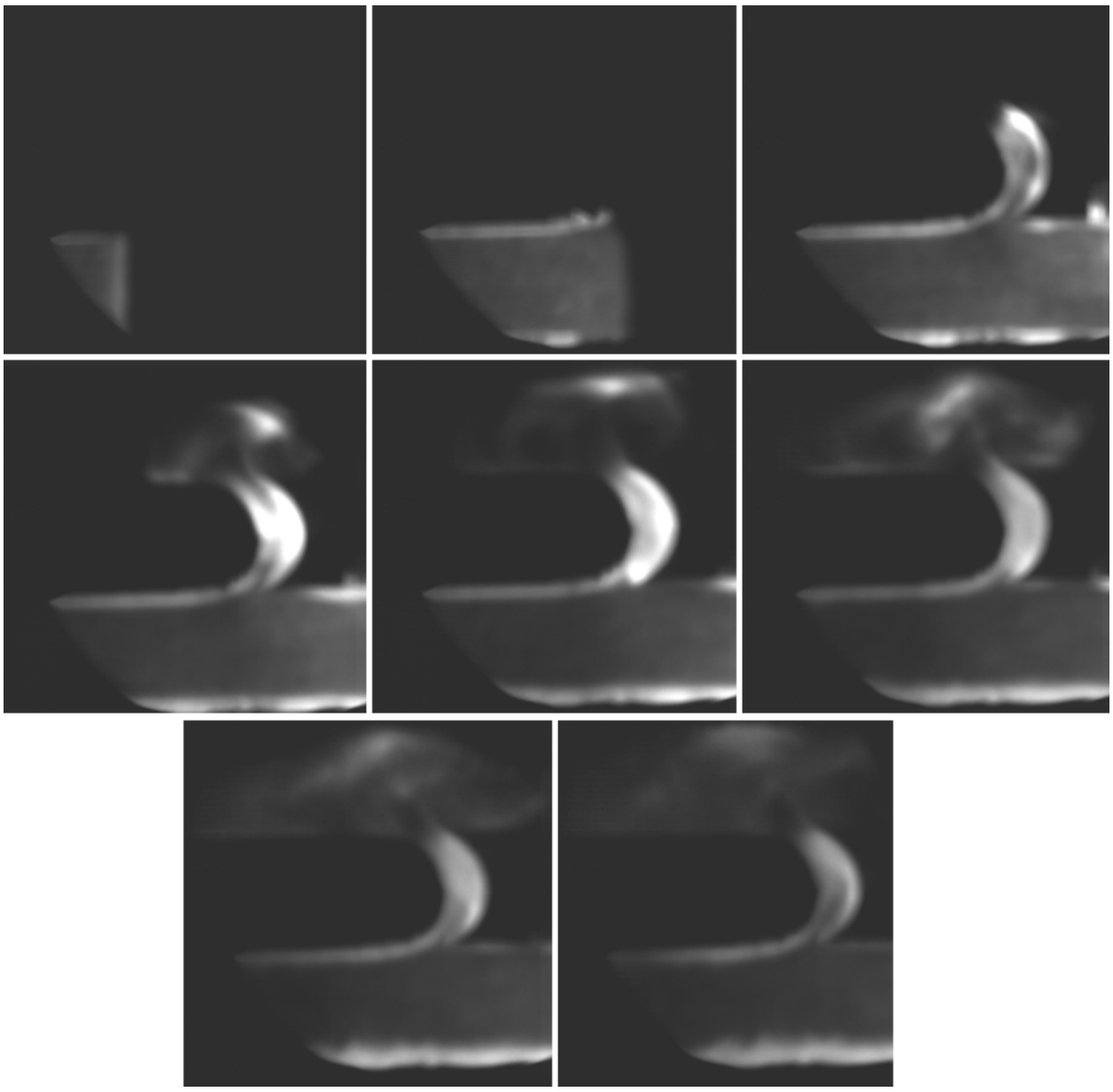

Figure A-3. Images of Run 6 on 10 February, detonation does not re-initiate. Cross-over is 0.7" in width. Schlieren light source has been turned off. Time is from left to right, top to bottom; detonation enters the bottom tube from left to right.

Figure A-3 is a picture of an unsuccessful transition through a 0.5" cross-over tube. A strong reaction is still seen in the cross-over tube but upon exit there is only a small bright spot which does not have sufficient energy to cause a re-initiation at the top wall. This appears to be the only difference from runs that did re-transition at a 1.7" cross-over width. The structure of

the wave is similar to the cases in which re-initiation does occur. As the cross-over is narrowed, more pressure is required from the initial detonation to push the same high velocity waves through the cross-over as seen in cases that re-transitioned.

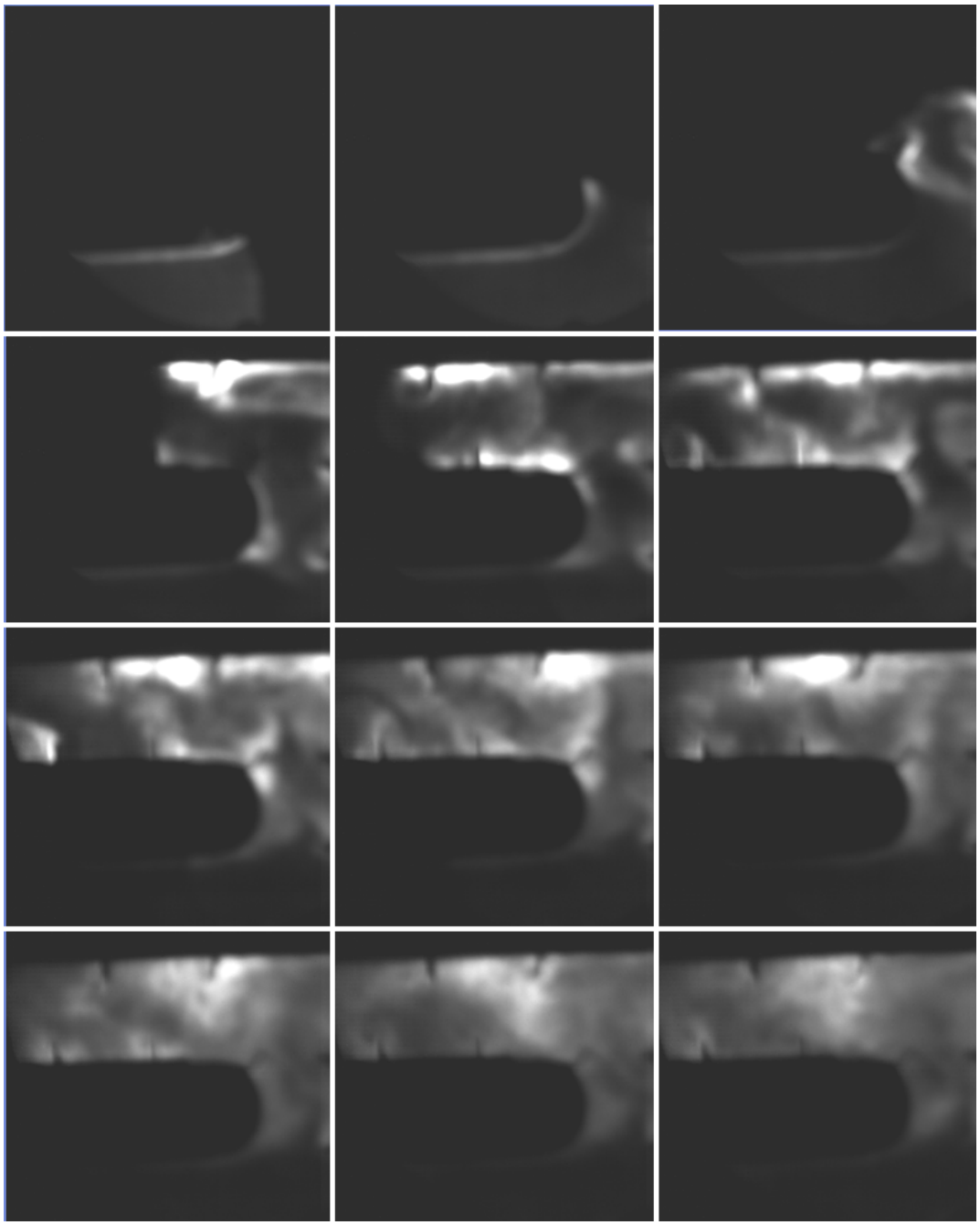

Figure A-4. Images of Run 6 on 11 February, detonation does not re-initiate. Cross-over is 1.7" in width. Schlieren light source has been turned off. Time is from left to right, top to bottom; detonation enters the bottom tube from left to right.

Figure A-4 is a good representation of how the obstacles trapped the high reaction areas. The obstacle in the cross-over tube does not seem to have an effect on creating a re-initiation site. However, as seen in the fourth frame, the first obstacle on the ceiling does produce a strong reflection. This reflection leads to another strong reflection on the bottom of tube 2, but mainly to the right of the first obstacle on the bottom. The shock wave and combustion front are continually moving to the left, any stoppage or slow down of these strong reaction areas are not able to help the re-transition to a detonation. In frames 5-10 it can be easily seen that the bright spot travels back and forth along the top, between the two obstacles. Note that the first obstacle on the top has a gap in it.

## Appendix B. Ion probe discussion

The wave speeds calculated from the ion probes and data reduction program were not reliable for the probes positioned in the test section (Fig. 30). Up to 40% of the wave speeds calculations returned were negative values or infinite values. This implies the combustion wave arrived at an ion probe pair at the same time, the voltage drop could not be detected by data reduction program or a probe upstream (further from the cross-over tube) was reached before a probe downstream (closer to the cross-over tube)

The ion probes seem to work well for detonations traveling at CJ speed for either the 10 inch probes spacing or the 1.5 inch spacing. Once the combustion front slowed to less than 1200 m/s there was significant variation in the calculated wave speeds. This is most likely because of the turbulent and three dimensional nature of the combustion zone when it is traveling as a high speed deflagration.

Due to the diffraction and expansion of the combustion wave the portion of the wave near the outside of the wall had significant curvature to it. The velocity vectors of the gases near the outside wall are mainly in the y-direction (Fig. 19), therefore as the combustion front continues to expand in the x-direction, parts of the wave just below the top wall of tube 2 may be traveling faster and will hit the next ion probe upstream at near same time as the combustion front attached to the outside wall hits the previous ion probe.

The problem did not change if wave speeds were calculated for probes far apart from one another, i.e. probes 3-6 in Fig. 30. Even when the camera wave speed calculations showed relatively constant wave speeds for consecutive detonations, the ion probe measurements were not constant, be it an accurate or inaccurate speed.

## Appendix C. Test Matrices

Table C-1. Test matrix for 2nd test series using the custom camshaft and varying cross-over geometries

| Date | Overall Run # | Run # | Fuel | Delay (ms) | Geometry | x-over width (in) | Equivalence Ratio | Fill Fraction | Purge Fraction |
|---|---|---|---|---|---|---|---|---|---|
| 2-Dec | 1 | 1 | Hydrogen | 2.4 | Square | 2 | 1 | 1 | 0.5 |
| | 2 | 2 | Hydrogen | 6.4 | Square | 2 | 1.1 | 1.1 | 0.5 |
| | 3 | 3 | Hydrogen | 2.4 | Square | 2 | 1.1 | 1.1 | 0.5 |
| | 4 | 4 | Hydrogen | 2.4 | Square | 1.5 | 1.1 | 1.1 | 0.5 |
| | 5 | 5 | Hydrogen | 2.4 | Square | 1.5 | 1.1 | 1.1 | 0.5 |
| | 6 | 6 | Hydrogen | 2.4 | Square | 1 | 1.1 | 1.1 | 0.5 |
| | 7 | 7 | Hydrogen | 2.4 | Square | 1 | 1.1 | 1.1 | 0.5 |
| | 8 | 8 | Hydrogen | 2.4 | Square | 0.5 | 1.1 | 1.1 | 0.5 |
| | 9 | 9 | Ethylene | 6.4 | Square | 0.5 | 1.2 | 1.1 | 0.5 |
| | 10 | 10 | Ethylene | 6.4 | Square | 1 | 1.2 | 1.1 | 0.5 |
| | 11 | 11 | Ethylene | 6.4 | Square | 1.5 | 1.2 | 1.1 | 0.5 |
| | 12 | 12 | Ethylene | 6.4 | Square | 2 | 1.2 | 1.1 | 0.5 |

Table C-2. Continued test matrix for 2nd test series using the custom camshaft and varying cross-over geometries

| Date | Overall Run # | Run # | Fuel | Delay (ms) | Geometry | x-over leng (in) | Equivalence Ratio | Fill Fraction | Purge Fraction |
|---|---|---|---|---|---|---|---|---|---|
| 3-Dec | 13 | 1 | Ethylene | 6.4 | S | 1.5 | 1.2 | 1.1 | 0.5 |
| | 14 | 2 | Ethylene | 6.4 | S | 1 | 1.2 | 1.1 | 0.5 |
| | 15 | 3 | Ethylene | 6.4 | S | 1.7 | 1.2 | 1.1 | 0.5 |
| | 16 | 4 | Ethylene | 6.4 | S | 0.5 | 1.2 | 1.1 | 0.5 |
| | 17 | 5 | Hydrogen | 6.4 | S | 0.5 | 1.1 | 1.1 | 0.5 |
| | 18 | 6 | Hydrogen | 6.4 | S | 1.7 | 1.1 | 1.1 | 0.5 |
| | 19 | 7 | Hydrogen | 6.4 | S | 1.5 | 1.1 | 1.1 | 0.5 |
| | 20 | 8 | Hydrogen | 6.4 | S | 1 | 1.1 | 1.1 | 0.5 |
| | 21 | 9 | Hydrogen | 2.4 | U | 1.7 | 1.1 | 1.1 | 0.5 |
| | 22 | 10 | Hydrogen | 2.4 | U | 1.5 | 1.1 | 1.1 | 0.5 |
| | 23 | 11 | Hydrogen | 2.4 | U | 1 | 1.1 | 1.1 | 0.5 |
| | 24 | 12 | Hydrogen | 2.4 | U | 1 | 1.1 | 1.1 | 0.5 |
| 6-Dec | 25 | 1 | Hydrogen | 2.4 | U | 1.5 | 1.1 | 1.1 | 0.5 |
| | 26 | 3* | Hydrogen | 2.4 | U | 1.5 | 1.1 | 1.5 | 0.5 |
| 20-Dec | 27 | 1 | Hydrogen | 2.4 | mod U | 1.7 | 1.1 | 1.1 | 0.5 |
| | 28 | 3* | Hydrogen | 2.4 | mod U | 1.5 | 1.1 | 1.1 | 0.5 |
| | 29 | 4 | Hydrogen | 2.4 | mod U | 1 | 1.1 | 1.1 | 0.5 |

*Run number 2 for testing on 6-Dec and 20 Dec did not provide useful data and has been omitted

Table C-3. Test matrix for 3rd test series using varying cross-over geometries and obstacles in the test section

| Date | Overall Run # | Run # | Fuel | Delay (ms) | Geometry | x-over width (in) | View | Equivalence Ratio | Fill Fraction | Purge Fraction | Nozzle |
|---|---|---|---|---|---|---|---|---|---|---|---|
| 10-Feb | 1 | 1 | Hydrogen | 2.4 | U | 1.7 | x-over | 1.1 | 1.2 | 0.5 | .5" |
| | 2 | 2 | Hydrogen | 2.4 | U | 1.7 | x-over | 1.1 | 1.3 | 0.5 | .5" |
| | 3 | 3 | Hydrogen | 2.4 | U | 1.7 | x-over | 1.1 | 1.3 | 0.5 | .5" |
| | 4 | 4 | Hydrogen | 2.4 | U | 1.2 | x-over | 1.1 | 1.3 | 0.5 | .5" |
| | 5 | 5 | Hydrogen | 2.4 | U | 0.7 | x-over | 1.1 | 1.3 | 0.5 | .5" |
| | 6 | 6 | Hydrogen | 2.4 | U | 0.7 | x-over | 1.1 | 1.3 | 0.5 | .5" |
| | 7 | 7 | Hydrogen | 2.4 | U | 0.7 | upstream | 1.1 | 1.3 | 0.5 | .5" |
| | 8 | 8 | Hydrogen | 2.4 | U | 1.2 | upstream | 1.1 | 1.3 | 0.5 | .5" |
| | 9 | 9 | Hydrogen | 2.4 | U | 1.7 | upstream | 1.1 | 1.3 | 0.5 | .5" |
| | 10 | 10 | Hydrogen | 2.4 | U | 1.7 | upstream | 1.1 | 1.3 | 0.5 | .5" |
| | 11 | 11 | Hydrogen | 2.4 | U | 1.7 | upstream | 1.1 | 1.3 | 0.5 | 1" |
| | 12 | 12 | Hydrogen | 2.4 | U | 1.7 | upstream | 1.1 | 1.3 | 0.5 | None |
| | 13 | 13 | Hydrogen | 2.4 | U | 1.7 | upstream | 1.1 | 1.1 | 0.5 | 1" |
| 11-Feb | 14 | 1 | Hydrogen | 2.4 | U w/obs | 1.7 | upstream | 1.1 | 1.3 | 0.5 | 1" |
| | 15 | 2 | Hydrogen | 2.4 | U w/obs | 1.7 | upstream | 1.1 | 1.3 | 0.5 | .5" |
| | 16 | 3 | Hydrogen | 2.4 | U w/obs | 1.2 | upstream | 1.1 | 1.3 | 0.5 | .5" |
| | 17 | 4 | Hydrogen | 2.4 | U w/obs | 1.2 | x-over | 1.1 | 1.3 | 0.5 | .5" |
| | 18 | 5 | Hydrogen | 2.4 | U w/obs | 1.7 | x-over | 1.1 | 1.3 | 0.5 | .5" |
| | 19 | 6 | Hydrogen | 2.4 | U w/obs | 1.7 | x-over | 1.1 | 1.3 | 0.5 | .5" |
| | 20 | 7 | Hydrogen | 2.4 | U w/obs* | 1.7 | x-over | 1.1 | 1.3 | 0.5 | .5" |
| | 21 | 8 | Hydrogen | 2.4 | U | 1.7 | x-over | 1.1 | 1.3 | 0.5 | .5" |
| | 22 | 9 | Hydrogen | 2.4 | U | 1.7 | x-over | 1.1 | 1.3 | 0.5 | .5" |
| | 23 | 10 | Hydrogen | 2.4 | U | 1.7 | x-over | 1.1 | 1.3 | 0.5 | .5" |
| | 24 | 11 | Hydrogen | 2.4 | D** | 1.7 | x-over | 1.1 | 1.3 | 0.5 | .5" |

*cross-over obstacle taken off

**U geometry removed from right side, semi-circle on left side remained

# REPORT DOCUMENTATION PAGE

*Form Approved*
*OMB No. 074-0188*



**PLEASE DO NOT RETURN YOUR FORM TO THE ABOVE ADDRESS.**

| **1. REPORT DATE** *(DD-MM-YYYY)* | **2. REPORT TYPE** | **3. DATES COVERED** *(From – To)* |
|---|---|---|
| 24-03-2011 | Master's Thesis | SEP 2009 – MAR 2011 |

**4. TITLE AND SUBTITLE**

Detonation Propagation Through Ducts in a Pulsed Detonation Engine

**5a. CONTRACT NUMBER**

**5b. GRANT NUMBER**

**5c. PROGRAM ELEMENT NUMBER**

**6. AUTHOR(S)**

Jeffrey M. Nielsen, Capt, USAF

**5d. PROJECT NUMBER**

**5e. TASK NUMBER**

**5f. WORK UNIT NUMBER**

**7. PERFORMING ORGANIZATION NAMES(S) AND ADDRESS(S)**
Air Force Institute of Technology
Graduate School of Engineering and Management (AFIT/EN)
2950 Hobson Way
WPAFB OH 45433-7765

**8. PERFORMING ORGANIZATION REPORT NUMBER**

AFIT/GAE/ENY/11-M21

**9. SPONSORING/MONITORING AGENCY NAME(S) AND ADDRESS(ES)**
Attn: Dr. Frederick Schauer
Air Force Research Laboratory
Propulsion Directorate, Turbine Engine Division, Combustion Branch
Bldg 71A, D-Bay, 7th St.
Wright Patterson AFB, OH 45433-7251
DSN 785-6462, frederick.schauer@wpafb.af.mil

**10. SPONSOR/MONITOR'S ACRONYM(S)**
AFRL/RZTC

**11. SPONSOR/MONITOR'S REPORT NUMBER(S)**

**12. DISTRIBUTION/AVAILABILITY STATEMENT**
Approved for public release, distribution unlimited

**13. SUPPLEMENTARY NOTES**
This material is declared a work of the U.S. Government and is not subject to copyright protection in the United States.

**14. ABSTRACT**
Development of a continuously operating pulsed detonation engine (PDE) without a high energy ignition system or a deflagration-to- detonation transition (DDT) device will increase engine efficiency, reduce cost, improve performance, and reduce weight. This report is a study of configurations that allow a consistent and predictable transition of a detonation from one detonation tube to second tube. The intent was, via visualization of detonation propagation through a cross-over tube, to develop a cross-over passage leading to minimization of energy losses and effective and repeatable tube-to-tube initiation. Detonation tube cross-over width, cross-over geometry and fuels were varied to determine their effect on tube-to-tube detonation initiation. The cross-over detonations studied decoupled into and out of the cross-over tube due to propagation as subcritical spherical detonations. It was shown that the mechanism of shock reflection could be used to transition the spherical detonation back to a planar detonation.

**15. SUBJECT TERMS**
Detonation, Pulsed, Engine, Shock wave, Propagation, Cross-over, Wave speed, Combustion, Chapman-Jouguet, Schlieren, Reflection, Re-initiation

| **16. SECURITY CLASSIFICATION OF:** | | | **17. LIMITATION OF ABSTRACT** | **18. NUMBER OF PAGES** | **19a. NAME OF RESPONSIBLE PERSON** |
|---|---|---|---|---|---|
| Unclassified | | | | | Paul I. King |
| **a. REPORT** | **b. ABSTRACT** | **c. THIS PAGE** | UU | 88 | **19b. TELEPHONE NUMBER** |
| U | U | U | | | (937) 255-3636, ext 4628 paul.king@afit.edu |

**Standard Form 298 (Rev. 8-98)**
Prescribed by ANSI Std. Z39-18

*Form Approved*
*OMB No. 074-0188*